Mechanical Engineering Department

Nanosilver Doped Poly-Phenylene-Sulfide Polymer Conductor

Mohammad Asyraf bin Mohammad Hatta

This thesis is presented for the Degree of

Master of Philosophy (Mechanical Engineering)

of

Curtin University

MAY 2019

DECLARATION

To the best of my knowledge and belief this thesis entitled "*Doping Concentration Influence of Electrical Behaviour of Nanosilver Doped Conductive Polymer*" contains no material previously published by any other person except where due acknowledgment has been made. This thesis contains no material which has been accepted for the award of any other degree or diploma in any university.

Signature : …….

Name : MOHAMMAD ASYRAF BIN MOHAMMAD HATTA

DATE : 23rd MAY 2019

THESIS COMMITTEE

Chairperson : Associate Professor Dr. Perumal Kumar

Supervisor : Associate Professor Dr. Sujan Debnath

Co-Supervisor 1 : Dr. Mahmood Anwar

Co-Supervisor 2 : Professor Dr. Michael K. Danquah

Associate Supervisor : Professor Dr. Izman Sudin

SUBMISSION LETTER

LOT 5221, LORONG 3B-1D,
DESA INDAH 3, BDR BARU PERMYJAYA, 98000,
MIRI, SARAWAK,
MALAYSIA.

23RD MAY 2019

The Chairperson,
Department of Mechanical Engineering,
Curtin University Malaysia,
CDT250, 98009 Miri,
Sarawak, Malaysia.

Dear Sir,

I submit this thesis entitled "*Nanosilver Doped Poly-Phenylene Sulfide Polymer Conductor"* for the fulfilment of the Master of Philosophy Program in Mechanical Engineering.

Yours faithfully,

Mohammad Asyraf bin Mohammad Hatta

18787154

"We hereby declared that we have read this thesis and in our opinion this thesis is sufficient in terms of scope and quality for the award of Master of Philosophy (Mechanical Engineering)"

On behalf of thesis committee,

Signature	:
Name of Supervisor	:ASSOC. PROF. DR. SUJAN DEBNATH
Date	:23RD MAY 2019

Signature	: …….
Name of Co- Supervisor	:DR. MAHMOOD ANWAR
Date	:23RD MAY 2019

Dedicated to my beloved wife and children, to whom I owe the most during the completion of this thesis and for the endless support. To my parents of whom had me a person I am today.

ACKNOWLEDGEMENT

I would first like to thank my research supervisors, Associate Professor Dr Sujan Debnath of Mechanical Engineering Department and especially Dr. Mahmood Anwar of Mechanical Engineering Department at Curtin University, Sarawak Campus. Their consistent guidance on the research journey, wisdom and lessons on be in life lessons and undertaking of this study is utmost appreciated of all.

Secondly, many thanks are due to Prof. Dr Perumal Kumar of the Mechanical Engineering Department at Curtin University, Sarawak Campus as the Chairperson of my Thesis Committee. Also, I extend my upmost gratitude to Prof. Dr Michael K. Danquah for his highly beneficial input on the early works of this thesis and candidacy. Their particularity and comments along the way of this research had inspired tremendous inputs and improvement along the way.

I would also like to acknowledge Prof. Dr. Marcus Man Kon Lee, former Dean of Curtin Sarawak Graduate School and Prof. Dr Clement Kuek current Dean of Curtin Sarawak Garduate School. Although our meetings are short, their support and advises will forever instilled in my mind as I continue my efforts towards achieving my goals.

Finally, I must express my very profound gratitude to my parents and to my little family especially my wife for providing with unfailing support throughout my years of study and through the process of researching and writing this thesis. This accomplishment would not have been possible without their sacrifice of time and effort. Thank you.

ABSTRACT

Conductive polymers had opened a new era of engineering materials particularly for microelectronics applications. This is due to their corrosion resistance and the capacity to conduct electricity. However, there still exist challenges for high voltage applications due to the lack of high electron charge transfer, resulting from low electrical conductivity of conductive polymers. This leads to significant energy loss during current transmission thus restricting the use for high voltage applications. This project investigated a novel method using nanosilver doped polyphenylene sulfide to enhance the potential of conductive polymers for high voltage applications. Nanosilver particles were doped intrinsically into poly (p-phenylene sulfide) (PPS) to enhance its charge transfer through molecular diffusion of electrical carriers in the polymer matrix. Preliminary works had identified the effective mixing speed of the solid solution which provide homogeneous organometallic hybrid. Investigation on threshold melting temperature was in the range 300ºC to 480ºC which led to identify the effective melting temperature at 420°C despite the identification of threshold melting temperature was at 380°C. Investigating the influence of nanosilver concentration in PPS revealed that there is a threshold at which a significant change of conductivity observed and reached to the metalloids conductivity value at $1.5x10^{-01}$ S/cm. Scanning Electron Microscopy micrographs and Fourier Transfrom Infra-Red analysis also further conforms such findings that the effects of the concentration on delocalization of the Π-bonds electron in the polymer chain. Thus, this study had established effective doping parameters for the development of highly conductive polymers towards high voltage applications with in-depth understanding of the doping mechanism.

LIST OF CONTENTS

ACKNOWLEDGEMENT I

Introduction 1

1.1 Research Background 1

1.2 Problem Statement 2

1.3 Objectives 3

1.4 Scope of Study 3

1.5 Significance of Study 4

1.6 Introduction Summary 4

Literature Review 5

2.1 Conductive Polymers 5

2.1.1 Conduction Mechanisms in Conductive Polymers 7

2.2 Poly (p-phenylene Sulfide) 10

2.3 Nanomaterials as dopant for conductive polymers 14

2.4 Silver Nano Particles 15

2.5 Critical Review 18

2.5.1 PPS doped with chemical dopants 19

2.5.2 PPS doping to improve electrical conductivity 23

Materials and Methodology 30

3.1 Overall Methodology 30

3.2 Materials 33

3.3 Preliminary Experiments 33

3.3.1 Solid Solution Mixing Speed 33

3.3.2 Threshold Melting Temperature 34

3.4 Structural Properties at Various Melting Point of Nanosilver Doped PPS 35

3.5 Characterization 36

3.6 Electrical Behavior Testing 36

Results and Discussion 38

4.1 General Introduction 38

4.2 Preliminary Experiments 39

4.2.1 Solid Solution Mixing Speed 39

4.2.2 Structural Properties at Various Melting Point of Nanosilver Doped PPS 45

4.2.3 Electrical Behavior 49

4.3 Influence of Doping Concentration on Nanosilver Doped PPS 50

4.3.1 Morphology 50

4.3.2 Electrical Behavior 58

4.3.3 FTIR Spectra Analysis 61

Conclusion 65

5.1 General Conclusion 65

5.2 Specific Conclusion 68

5.3 Future Work 68

5.4 References 70

LIST OF FIGURES

Figure 2.1.1. Chemical structure of Polyacetylene (PAC) 7

Figure 2.1.2: Chemical structure of Polyphenylenevinylene (PPV) 7

Figure 2.1.3: The hybridization of $2s^2$ and $2p^2$ electrons into sp^2 hybrid orbitals. 8

Figure 2.1.4: The carbon atoms in phenyl rings has one p-orbitals of electrons each. The orbitals are delocalized and form the delocalized orbitals above and under the ring[33]. 9

Figure 2.1.5: (a) σ-bond and (b) Π-bonds in acetylene [35]. (c) In polyacetylene, the polymer chains are made of these bonds in alternating manner. 10

Figure 2.2.1: Poly (p-phenylene sulfide) 11

Figure 3.1.1: Overall Experimental Methodology 32

Figure 3.1.2 32

Figure 3.6.1: Electrical Behavior Test 37

Figure 4.2.1: Micrography images of variable mixing speed of solid solution for nanosilver doped PPS; (a) 60rpm, (b) 80rpm, (c) 100rpm, (d) 120rpm and (e) 140rpm. 41

Figure 4.2.2 (a) The typical conditions of incomplete melting of solid solution below the threshold temperature (b) The complete organometal hybrid melted above threshold temperature of 380°C 43

Figure 4.2.3: Graph of Melting Temperature vs Melting Start Time. Melting start time reduced significantly at 340ºC and stabilized at 380ºC to 480ºC. 44

Figure 4.2.4: SEM Image of ST400. Some coagulations can be found (red circles) indicating incomplete melting of the PPS at 400ºC. 46

Figure 4.2.5: SEM image of ST420. Arrow shows nucleation of which starting to form at this melting temperature of 420ºC. 47

Figure 4.2.6: SEM images of (a) ST440, (b) ST460 and (c) ST480. Arrows shows the porosities that formed through this temperature range (440-480ºC). 48

Figure 4.2.7: Electrical conductivity of nanosilver doped PPS as a function of melting temperature. 49

Figure 4.3.1: Morphology of pure PPS (SR-0). Smooth surface shows no trace of nanosilver. 51

Figure 4.3.2: Image of SR-10 of PPS with 10% nanosilver content. Dismal sized bright spots without apparent nucleation could be identified. 52

Figure 4.3.3: Image of SR-10 of PPS with 20% nanosilver content. Obvious bright spots of the nanosilver in clusters are observed. 52

Figure 4.3.4: Image of SR-30 of PPS with 30% nanosilver content. Larger localized clusters of nanosilver are observed. 53

Figure 4.3.5: Image of SR-40 of PPS with 40% nanosilver content. Very distinct nucleation formations which the borders of the clusters could be observed unlike in the hybrids below 30%. 54

Figure 4.3.6: Image of SR-50 of PPS with 50% nanosilver content. Well-established nucleations clearly seen as indication of saturation. 54

Figure 4.3.7: Image of SR-60 of PPS with 60% nanosilver content. Surface are dominated by combined nucleation of nanosilver. 55

Figure 4.3.8: The summary of SEM images of samples (a) SR-0, (b) SR-10, (c) SR-20, (d) SR-30, (e) SR-40, (f) SR-50 and (g) SR-60. Nucleation are

formed progressively in size from 30-50% until saturation at 60% of nanosilver. 57

Figure 4.3.9: Electrical conductivity of nanosilver doped PPS as a function of nanosilver concentrations. 60

Figure 4.3.10: FTIR Spectra of nanosilver-PPS hybrids in various concentrations. Blue dashed lines show the trend of the FTIR absorption rate as the infrared wavelength reduced from 4000nm to 700nm. 62

Figure 4.3.11: The FTIR spectra of pure vs doped PPS [69] 63

LIST OF TABLES

Table 1: Examples of extensively researched conductive polymers [12, 32]. 6

Table 2: Properties of PPS [32, 37, 47]. 12

Table 3: Properties of silver [58, 59]. 16

Table 4: Electron affinity and ionization energy of PPS elements, silver and copper [59, 62, 63]. 18

Table 5: Summary of Critical Review on PPS researches. 26

Table 6: Critical review on PPS doped with nanomaterials and micro-copper 28

Table 7: Mixture Melting Temperature Experiment Observation 43

Table 8: Concentration vs Mean Conductivity/Resistance Values 59

ABBREVIATIONS

Ag	-	Silver
AgNPs	-	Silver nano particles
PPS	-	Poly (p-phenylene Sulfide)
S	-	Siemens
Cm	-	centimeter
CH_4	-	Methane
Be	-	Beryllium
N	-	Nitrogen
O	-	Oxygen
H	-	Hydrogen
F	-	Fluorine
Ne	-	Neon
MWNCT	-	Multi-Walled Carbon Nanotubes

CHAPTER 1

INTRODUCTION

1.1 Research Background

Almost all heavy industries such as power generation, marine and, oil and gas deals with high voltage applications. In these applications, metals play an important role as electric conductors. Metals are known as good electric conductors, however almost every metal is corrosive, especially if the metal is exposed to corrosive environment for a significant period. Metals are highly reactive due to their conductive properties which enables them to possess high electron mobility. Good electric conductors include; copper, gold and silver. However, all of them are corrosive.

Polymers by nature are corrosive resistant due to strong covalent bonds and lack of free electron mobility. Generally, polymers are long chains of repeating units known as monomer and this provides properties significantly different from the monomer. Examples of polymers in everyday use are polyethylene (PE), polypropylene (PP) and polystyrene (PS) [1]. They are used for packaging purposes and molding with applications in fabricating automotive parts and household

appliances [2]. However, some polymers exhibit electrical properties such as electrical conductivity. These polymers are conductive polymer [3].

1.2 Problem Statement

Conductive polymers are challenged with limited charge transfer, and this has affected applications excluding microelectronics. For higher voltage applications, charge mobility is essential to allow high conductivity and reduce transmission loss. PPS has been known to be doped to enhance the conductivity with various material such as copper and carbon nanotubes [4, 5]. However, due to highest conductivity, silver is the most promising candidate [6]. Nevertheless, by reducing the size of silver to nanoparticles, the diffusion of nanosilver could be most effective. Nanosilver has been used in doping other types of conductive polymers such as polypyrole and PEDOT:PSS to enhance their electrical conductivity. PPS also has huge potential to be doped with nanosilver to produce high conductive polymer [7]. Nevertheless, studies reporting the use of nanosilver with PPS to improve the polymer electrical properties is scarce in literature. Introducing nanosilver in PPS, the Π-bond delocalization could be promoted where nanosilver has the affinity to distort the C-S bond in that PPS polymer chain due to the excitation of Π-electrons [8, 9]. Hence, further delocalized Π-bond leads to create additional pathways for charge mobility. This phenomenon is expected to potentially enhance the polymer electrical conductivity of the nanosilver doped PPS organometallic hybrid.

1.3 Objectives

The overall objective of this study is to increase the electrical conductivity of the polymer conductor to suit high voltage application. The specific objectives of this study are:

1. To determine effective doping process parameters comprising mixing speed of solid solution and melting temperature in order to analyze the diffusion behavior of nanosilver in the polymer matrix during doping.
2. To identify effective threshold doping concentration of nanosilver particles with PPS to allow for massive Π-electron delocalization to overcome the electrical insulation barrier into conductive region of PPS.
3. To characterize the electrical behavior of newly developed hybrid material and correlate to doping process.

1.4 Scope of Study

The scopes of this study are as follows:

1. This study focused on few key parameters such as effective mixing speed of nano particle in PPS, threshold melting temperature and effective concentration of nano particles in polymer powder.
2. This research is limited to PPS as the doped conductive polymer and silver nano particle as the dopant.

3. Corrosion test is not within the scope since polymers are corrosion resistant material.
4. Mechanical testing of PPS is not be covered in this study.

1.5 Significance of Study

The significance of this study is to determine the effective parameter of nanosilver into the PPS polymer matrix to allow high charge transfer capability much required in high-voltage transmission in marine and energy transfer in highly corrosive environment.

1.6 Introduction Summary

In the following section, the type of polymers and their applications would be discussed in detail. The studies done on conductive polymer would be elaborated to reveal the research gap regarding nanoparticle doped PPS.

CHAPTER 2

LITERATURE REVIEW

2.1 Conductive Polymers

Polymers are well known as an electric insulating agent as they have limited free-moving electrons. However, there are a group of polymers known as conductive polymers. Several conductive polymers include polypyrrole (PPy), polyaniline (PANI) and polythiophene derivative, poly (3,4-ethylenedioxythiophene) [10]. Table 2.1.1 illustrates the commonly researched conductive polymers currently. Polypyrrole is well known for its good chemical stability and reasonably high conductivity under physiological conditions [11, 12]. Today, polypyrrole are useful as corrosion protection, in fuel cells construction and computer display. In medical field, polypyrrole also found application as microsurgical tools, biosensors, drug delivery system, neural probes, nerve guidance channels, blood conduits and as a biomaterial

in neural tissue engineering due to flexibility [13-21]. Polyaniline is used in biosensors, neural probes, controlled drug delivery and tissue engineering applications [22-26]. Poly (3,4-ethylenedioxythiophene) is mainly used in bio sensing and bioengineering applications such as neural electrodes, nerve grafts and heart muscle patches [7, 27-29]. Polyacetylene (PAC) and Polyphenylenevinylene (PPV) has limited application in microelectronics [30, 31]. These polymers allow the mobility of the charges by having conjugated backbones, or in other words, having alternated single and double bonds between their carbon atoms [12].

Table 2.1.1: Examples of extensively researched conductive polymers [12, 32].

Content of main chains	**Carbon and Hydrogen atoms only**	**Carbon, Hydrogen and Heteroatoms**			
		Sulfur (S)		**Nitrogen (N)**	
Aromatic Cycle		inside aromatic cycle	outside aromatic cycle	inside aromatic cycle	outside aromatic cycle
	1.polyphenylenes 2.polypyrenes 3.polynaphthalenes 4.poly(fluorene)s 5.polyazulenes	1.poly(thiophene)s (PT) 2.poly(3,4-ethylenedioxythiophene) PEDOT)	Polyphenylene sulfide (PPS)	1.poly(pyrrole)s (PPy) 2.polycarbazoles 3.pirlindoles 4.polyazepines	Polyaniline (PANI)

Double bonds only	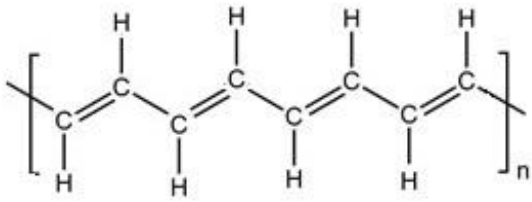 **Figure 2.1.1. Chemical structure of Polyacetylene (PAC)**
Both aromatic cycles and double bonds only	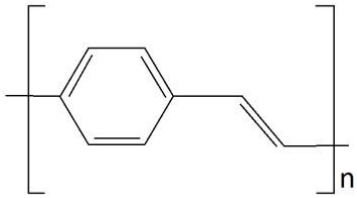 **Figure 2.1.2: Chemical structure of Polyphenylenevinylene (PPV)**

2.1.1 Conduction Mechanisms in Conductive Polymers

In understanding how conductivity happens in conductive polymers, the fundamentals of electrons orbitals and how it relates to the mobility of electron within the polymer chain must be understood.

2.1.1.1 Carbon Orbitals and Phenyl Ring Structure

It is important to know that most conductive polymers are organic compound which are hydrocarbons. In conductive polymers, carbon orbitals are made by forming hybridization of electron orbitals of their $2s^2$ and $2p^2$ into sp^2 orbitals (Figure 2.1.3).

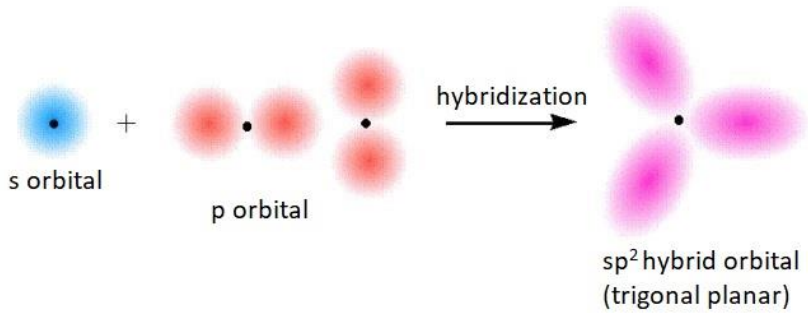

Figure 2.1.3: The hybridization of $2s^2$ and $2p^2$ electrons into sp^2 hybrid orbitals.

Moreover, some conductive polymers are made of phenyl rings like PPS. In this case, each of the six carbon atoms has p-orbital and sp^2 orbitals forming a circle or ring. Due to the proximity and repulsion forces between the orbitals, the p-orbital electrons are then becoming delocalized Π-bonds arranged in a circle. The Π-bond are further delocalized in the phenyl ring [33]. The structure is best described by illustration in Figure 2.1.4.

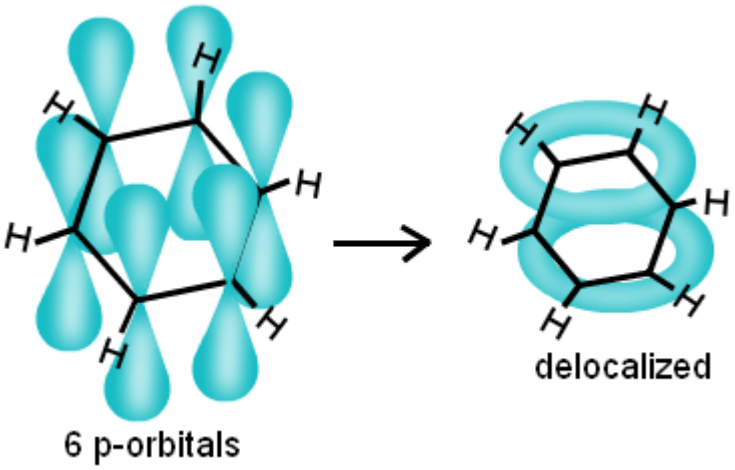

Figure 2.1.4: The carbon atoms in phenyl rings has one p-orbitals of electrons each. The orbitals are delocalized and form the delocalized orbitals above and under the ring[33].

2.1.1.2 Conjugated Backbone; Alternating Single and Double Bonds

The main character in conductive polymers which allows for charge movements are conjugated backbones. The backbones consist of alternating single and double bonds. These are made of σ-bonds and Π-bonds, for instance, when two acetylene molecules started to form a polymer, as illustrated in Figure 2.1.5. The σ-bonds are generally stronger compared to Π-bonds and requires high amount of energy to break. However, in these polymers, the atoms are also bonded by the comparatively weaker Π-bond. These weak Π-bond are delocalized which makes conjugated polymer as conductive [34]. Dopants, when added into the pristine (pure) polymers, enhances the delocalization of the Π-electrons and thus increases the conductivity.

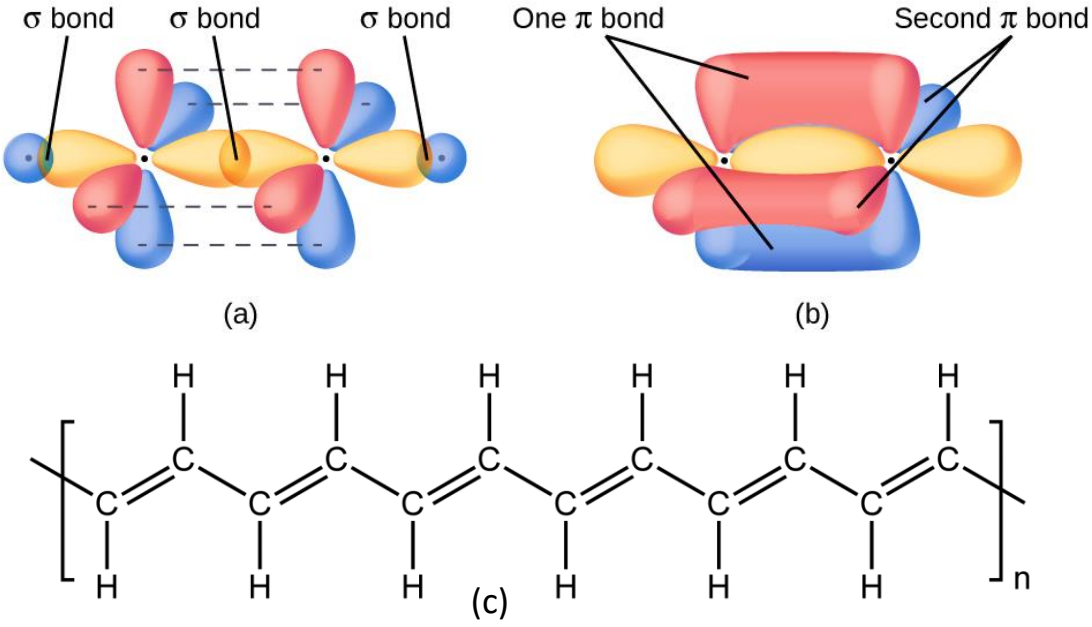

Figure 2.1.5: (a) σ-bond and (b) Π-bonds in acetylene [35]. (c) In polyacetylene, the polymer chains are made of these bonds in alternating manner.

2.2 Poly (p-phenylene Sulfide)

Among the conductive polymers, Poly (p-phenylene sulfide), also written as poly (1, 4-phenylene sulfide) and poly (para-phenylene sulfide) had been known to be an excellent engineering polymer. PPS structure is a repetition of a phenyl ring attached with a heteroatom of sulfur, thus, it is a heteroatom-linked polyphenylenes as shown in Figure 2.2.1. The chemical formula for a monomer of PPS is C_6H_5S.

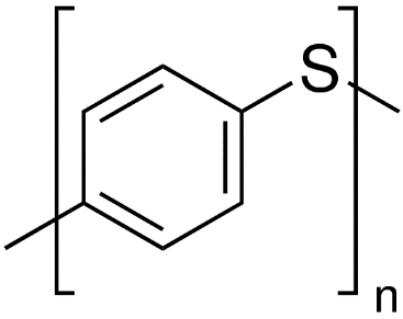

Figure 2.2.1: Poly (p-phenylene sulfide)

The preparation of PPS is a reaction of dichlorobenzene with sodium sulfide in a polar solvent such as N-methylpyrrolidin-2-one (NMP) [36-38]. PPS can be melt as well as solution processed [39], which renders it to be highly-preferred in manufacturing [40]. In addition to its thermosetting-thermoplastic characteristics, PPS displays very good thermal stability, insolubility, resistance to chemical environments, and natural flame resistance [1, 2, 41-44]. The thermodynamic melting temperature of PPS is at 295°C in atmospheric pressure and decomposes into various gaseous of carbon monoxides, carbon dioxides and hydrogen sulfide at temperature above 400°C [45, 46]. Other important properties of PPS are presented in Table 2.2.1.

Table 2.2.1: Properties of PPS [32, 37, 47].

Properties of Polyphenylene Sulfide	
Abbreviation	PPS
Melting Temperature	285-290°C
Glass Transition Temperature	150°C
Ionization Potential	~6.3eV
Specific Gravity	1.36g/cm^3
Hardness	95 (Rockwell M) 125 (Rockwell R)
Drying Time	3-6 hrs.
Drying Temperature	250-325°F (121-163°C)
Surface Resistivity	6.0-2.5 x 10^{15}

There are many research interests in PPS in recent years due to the mentioned properties, though the studies mostly involved fabrication of PPS as a composite component. Zeng et al. studied PPS-fiber composites for the application in gas sensors [44]. The study revealed that PPS resistance increases remarkably when exposed to organic vapors with low permittivity. Kalkar et al. attempted to enhance the moldability of PPS and its composite with thermotropic liquid crystalline polymer (TLCP), and achieved remarkable effects on PPS crystallization which shows that the polymer has shorter activation energy to nucleate at lower temperature but with heat of crystallization reduced overall [48]. There is also a study to improve thermal and mechanical properties of PPS composites produced by high-energy ball milling. The study shows that the introduction of polyimide filler contributed to the loss of

crystalline regions of the PPS matrix which sharply increased the recrystallization temperature [22]. In another research, Benlhachemi et al. used PPS as a component of a high temperature superconductor polymer composite and concluded that it is much more feasible to manufacture conductor polymer composites by using PPS than the previous attempt of using Low-Density Polyethylene (LDPE) [49]. However, these studies mainly focused on the mechanical performances of PPS rather than electrical properties such as electrical conductivity. This is due to the fact that pristine PPS had known to be an excellent electrically insulator as high as $10^{22}\,\Omega$ [22].

However, there are a few studies conducted regarding electrical properties of PPS recently. Taherian had proposed experimental and analytical model of electrical conductivity properties of polymer-based nanocomposites including PPS-graphene composites [50]. Experimental studies were conducted by Diez-Pascual et al. on electrical properties of carbon nanotubes/polyphenylene sulfide composites incorporating polyetherimide and inorganic fullerene-like nanoparticles namely SWCNTs [51]. It was found that at 0.1% loading, the composite remains insulating, before an abrupt increment of about ten orders of magnitude was observed in the range 0.1–0.5%. However, the conductivity rises gradually to ~10^{-3} S/cm due to further increase of SWCNTs. Goyal discussed about the sintering process of PPS-micro copper composite and investigated their thermal and electrical properties. [8]. This research work also found that the highest electrical conductivity was obtained at 60%

of Cu micro-copper at 4.2×10^{-7} S.cm^{-}1, which is improved by four orders of magnitude. However, further increment of micro-copper concentration resulted in drop of electrical conductivity.

2.3 Nanomaterials as dopant for conductive polymers

In recent years, the enhancement of various properties obtained from metal nanoparticles-polymer combinations have been drawn the focus of intense research [52]. The nanoparticles doping functions as a process that introduces the charge carriers into the polymer resulting in a conductive polymer. One example of nanocomposite would be polypyrrole nanotube-silver nanoparticle (PPy-NTs/Ag-NPs) nanocomposite. The study shows that the AC conductivity of the PPy-NTs/Ag-NPs nanocomposite had been significantly increased [53]. Saptarshi Dhibar et al. investigated on poly(aniline-co-pyrrole) multi-walled carbon-nanotubes that were doped with transition metals. In that study, chemical oxidative polymerization was utilized to fabricate copolymer of PANI and PPy for high performance supercapacitor electrode material [54]. Apart from that, graphene also have wide utilization as a dopant in conductive polymers. It is understood that graphene, with conductivity of electrical conductivity ($\sigma = 10^6$ ohm^{-1}cm^{-1}), it could improve the base polymer electrical behavior significantly [55]. Thus, Kandare et al. attempted at improving the thorough thickness electrical conductivity of fibre-reinforced polymer by inclusion of graphene nano platelets and silver nanoparticles/nanowires. It was found that at a

minimum of 70% improvement of conductivity was achieved in comparison of using graphene nano platelets alone [56]. These researches had utilized either compressing technique of polymer powders or chemical process using polyol to form nanocomposites.

Aside of compressing techniques and chemical process to form nanocomposite, another method called dual doping was also employed for through doping of nanoparticles into the structure of the polymer. Yu Song et al. experimented on the dual doping of polypyrrole on graphene sheets using electrochemical anchoring. In their research, pyrrole was electro-polymerized on the partially exfoliated graphene sheet. The cyclic charge/discharge stability of the polymer were improved by the synergistic effect with partially exfoliated graphene [57]. These studies had revealed the potential of nanomaterials to enhance the properties of conductive polymers. However, those studies had not addressed the usage of nanosilver to dope PPS for improvement of the polymer electrical conductivity.

2.4 Silver Nano Particles

Silver had been known as the highest conductive metal in its elemental form. It is due to the high charge mobility provided by its valence electron and subsequent electrons in its next lowest electron shell, the $4d^{10}$ orbitals. This high conductivity also can be explained by the large overlap of the Valence and Conductive Bands of silver,

where the electrons are free to move when the atoms of silver are close together, creating 'free electron gas' or Fermi gas [12, 58]. The electrical conductivity of silver is 6.30×10^7 S/m at 20 °C. Important properties of silver are illustrated in

Table 2.4.1.

Table 2.4.1: Properties of silver [58, 59].

Properties of silver	
Symbol	Ag
Appearance	Lustrous white metal
Group, Period	11,5
Atomic Number	47
Atomic Weight	107.87
Atomic Radius	144 pm
Covalent Radius	145±5 pm
Van der Waals Radius	172pm
Electronic Configuration	$[Kr]4d^{10}5s^1$
Valence Shell	2, 8, 18, 18, 1
Melting Temperature, T_m	1234.93K (961.78°C)
Boiling Temperature, T_b	2435K (2162°C)
Density	10.49 g/cm^3 @ 25°C 9.320 g/cm^3 @ T_m
Molar Heat Capacity	25.350 J/mol.K
Hardness	3.25 (Mohs Scale)

Nanoparticle defined by particles with diameter of less than 100nm in one of its largest dimension according to United States Environmental Protection Agency US-EPA [60]. The advantage of using nanoparticles is due to the ultra-small particle

size would mean larger amount of atoms are in contact with ambience and readily available for reaction [9]. Thus, the surface area per unit mass would be extra-large. Moreover, the ultra-small particle size enables the metal to diffuse into the structure of the polymer easily during the doping process. In this study, it is expected that the silver nanoparticles, when diffused effectively into the polymer matrix due to its very small size, will agitate the sulfur atom in the polymer chain.

For silver nanoparticle doped PPS, the valence electrons from nanoparticle jump into sulfur orbitals thus creating a double bond. The additions of the double bond into the polymer chain further enhance the delocalization of the electrons and introduce conjugation in the polymer chains. This is due to the lowest ionization potential (IP), also known as Ionization Energy (IE) of silver of 731kJ/mol in contrast to other atoms in the polymer [61]. Sulfur also has a high negative electron affinity (EA) of -200kJ/mol and have the highest tendency to attract the valence electron from silver apart from other element in the PPS [61]. This reactivity among sulfur and silver render high mobility of the electrons when there is an electrical potential across the silver-doped polymer length and thus will enhance the electrical conductivity of PPS. The comparison between PPS components atoms and silver in term of ionization energy and electron affinity are illustrated in Table 2.4.2.

. The tarnishing of silverware is a classic example of reaction between sulfur and silver, where black precipitate of Ag_2S produced on the surface of the silverwares

[59]. It is due to this interaction of silver and sulfur that enhance the electron mobility in the resulted organometallic hybrid.

Table 2.4.2: Electron affinity and ionization energy of PPS elements, silver and copper [59, 62, 63].

Element	Carbon	Sulfur	Silver	Copper
Electron Affinity, E_A	-153.9 kJ/mol	-200 kJ/mol	-125.6 kJ/mol	-118.4 kJ/mol
Ionization Energy, E_i	1086.5 kJ/mol	999.6 kJ/mol	731 kJ/mol	745.5 kJ/mol

2.5 Critical Review

This part of the discussion will concentrate on polyphenylene sulfide. Michael Rubner et al. in 1981 published a paper on the doping of PPS with nitrosyl salts. The doping ratios used in that research paper were varied with maximum concentration of nitrosyl salts at 38mol% [64]. However, it was found that the ratio that produced the highest conductivity was 36.3mol%. In 1983, N.E. Murthy et al. studied the structural changes during annealing of acceptor doping of PPS. The paper found that the crystallinity of the PPS film affects the conductivity of the polymer, with heavily doped unannealed sample having the conductivity of 0.18 S/cm whereas a film annealed at 125°C for 18 hours had a conductivity of 0.22 S/cm [65]. In 1984, Shizuo Tokito et al. studied the electrical conductivity and optical properties of PPS doped with several organic acceptors. The study discussed about the effects of doping PPS

with tetra-cyanothylene (TCNE), dicyanodichrolobenzoquinone (DDQ), *p*-chloranil and trinitrofluorenone (TNF). The results shows that of all four, only DDQ and TCNE increased the conductivity of PPS with a conductivity range between 10^{-9} and 10^{-11} S/cm. This is due to the fact that both organic acceptors have higher electron affinity. The molar ratio, expressed as mole dopant/mole PPS, found to achieve the highest conductivity of 0.145 for TCNE and 0.067 for DDQ [66]. In 1986, S. Kazama studied the molecular structure of sulfur trioxide (SO_3) doped PPS using proton nuclear magnetic resonance (^1H N.M.R.), Carbon-13 cross-polarizing magic-angle spectroscopy (C CP-MAS) nuclear magnetic resonance and infrared spectroscopy. The study found substantial modification of the polymer structure when doped with SO_3. The powder was heated to 100°C in one condition and room temperature doping in another. However, the conductivity enhancement was limited as mentioned in the research paper [67]. In 1992, C. Arbizzani et al. studied the electrochemical doping of PPS in concentrated sulfuric acid. The paper studied the cyclic voltammetry curves, cyclic voltabsorptiometry curve and electronic spectra of the doping matrix but made no mention of the resulting conductivity of the doped polymer [68].

2.5.1 PPS doped with chemical dopants

In 1986, Tsukamoto and Fukuda et al. reported on the conduction mechanism of doped polyphenylene sulfide, which studied the effects of doping PPS with tantalum

fluoride (TaF_5) in nitromethane solution. This research focused on the doping of PPS using X-ray photoelectron spectroscopy (XPS), infrared spectroscopy and Carbon-13 Nuclear Magnetic Spectroscopy (C-NMR). The XPS studies shows that the sulfur atoms were converted into radical cations. From the C-NMR study, which was measured using cross-polarizing magic-angle spectroscopy (CP-MAS), for a pure PPS film two peaks were observed at 135ppm and 127ppm whereas doped PPS saw a single peak at 132.1ppm. The single peak is due to the equalization of carbon atoms in the phenyl ring, which indicates that the electrons were delocalized in the polymer chain [69]. In the same year, D. R. Rueda et al. studied on the properties of PPS/PPP mixture doped with antimony pentafluoride, $SbCl_5$. The study found that for compound mixing with PPP greater than 20%, the conductivity increases significantly (within the range of 10^0 S/cm) with good electrical stability in nitrogen atmosphere [70]. P. Hruzka et al. in 1990 studied the nuclear magnetic relaxation in polyphenylene sulfide doped with $FeCl_3$. PPS was doped with $FeCl_3$ using two different methods, 1M of $FeCl_3$ and 0.1M $FeCl_3$ were added into nitromethane. This study discovered that PPS conductivity increased by multiple orders, peaking at 6×10^{-5} S/cm. The results also showed that conductivity of amorphous film was at least two orders of magnitude higher [71]. In 1989, Radhakrishnan et al. published a journal reporting the effects of doping PPS with iodine. It was found that doping iodine with pristine PPS (sintered at 285-290°C) only improved its conductivity marginally. In this study, adding copper phthalocyanine (CuPH) dramatically improved the conductivity of PPS doped with

iodine even at low concentration with the lowest resistivity at 30mol% of CuPH [72]. In 2011, R. K. Goyal et al. fabricated PPS/copper compound. The copper powder used was within the micro range and prepared in an ethanol solvent using ultrasonic bath for 10 minutes. Five different compositions of copper were used in the study, in the range of 0-75wt% with mixture compacting temperature at 100℃. The result exhibited that with the highest conductivity achieved at 60wt% (4.2×10^{-7} S/cm). However, conductivity decreased at 75wt%. Although metal particles are used, the copper are in micro size and the process employed is not involving of melting of PPS [8]. In 2016, Dandan Lian et al. published a report about enhancing the resistance against oxidation of PPS fibers with the addition of nanosized TiO_2-SiO_2 into its polymer matrix. The materials were prepared via melt spinning with masterbatch samples of 1.0, 2.0, 3.0 and 4.0wt% of effective TiO_2-SiO_2 with the PPS. The paper however did not mention about any effects on conductivity of polymer [73].

More recently, Y.F. Zhao et al. demonstrated on the preparation and properties of electrically conductive PPS-expanded graphite (EG) mixture. It is reported that the conductivity of PPS significantly improved with expanded graphite (EG) and ultra-sonicated expanded graphite (S-EG). At only 10% graphite composition, the conductivities were up to about 10^{-3} for EG and10^{-2} for S-EG [74]. In another research, Jinghui Yang et al. studied on the preparation and properties of PPS/multiwall carbon nanotube (MWCNT) compound mixture via melt compounding. The investigation

used a range of weight percentages of MWCNT (0.2, 0.5, 1, 2, 3, 5, 7, 9 and 11) melt blended with PPS powder. The electrical resistivity decreased in three stages during the carbon nanotube loading. The first stage showed gradual decrease in resistivity from 0.2 to 5wt% of CNT. A sharp decrease occurred between 5-7wt% (resistivity from 10^{-12} - 10^{-7} ohm/cm) but limited decrease noticed from 7-11wt%. This shows that 5-7wt% of CNT loading offers the lowest resistivity. However, the highest achieved conductivity occurred at 11wt% [75]. Arash Golchin et al. investigated the influence of counter surface topography on tribological behavior of PPS/carbon filler mixture [76]. Multiwalled carbon nanotube (MWCNT) was used at 3-wt%, carbon graphite flakes at 10wt% and special carbon fiber (SCF) at 15wt%. However, the experiments focused more on the surface mechanical properties such as friction and wear of the polymer/carbon filler matrix and not the electrical conductivity.

In 2016, Wei Luo et al. investigated the surface morphology and mechanical behavior of poly (p-phenylene sulfide) and polytetrafluoroethylene (PPS/PTFE) composites reinforced with carbon fiber. The experiments were performed via melt blending at the range of temperatures from 265℃ to 295℃ [77] [77]. Meanwhile, Shuling Deng et al. studied a novel method to strengthen PPS by means of nano diamond as a nucleating agent. The mixing ratio between PPS and nano diamond used in weight percentage were 100:0, 99.9:0.1, 99.5:0.5, 99:1, 98:1, and 97:1. The mixing process was done via a twin-screw extruder. The temperature used in the experiment

was in a range between 220-290℃. In another study, Diez-Pascual et al. investigated the effects on mechanical and electrical properties of carbon nanotubes/PPS composites with the addition of polyetherimide and inorganic fluorine-like nanoparticles [51]. The study was performed to investigate the dynamic mechanical behavior of the composites and to improve the composites' conductivity. The mixing process was done using a Haake Rheocord 90 extruder and the melting temperature used in the experiment was 320℃. These papers involved melt-processing via extruder machines and various melting temperatures. However, none of the nanoparticles used are nanometals such as nanosilver.

2.5.2 PPS doping to improve electrical conductivity

Other than nanoparticles, PPS has been known to work with chemical dopants such As F_5 and CF_3COOH, in gaseous and liquid form respectively to improve the polymer conductivity [10]. Tsukamoto et al. has found that PPS can be doped with TaF_5 in nitromethane solution to increase its conductivity to the range of 10^{-4} to 10^{-3} S/m [69]. PPS doped with strong electron acceptor such as ASF_5, can have electrical conductivity as high as 0.01 S/m. Films produced with ASF_3 solution of ASF_5-doped PPS proven to have electrical conductivity as high as 2 S/m as demonstrated by Shacklette et al. [39]. Nevertheless, Clarke et al. reported the doping of PPS with AsF_5 had increased the conductivity to the range of 0.01 – 0.1 S/m [40]. The effects of TaF_5-

doped PPS which were annealed uniaxially and biaxially had been further investigated for electrical conductivity by Ko et al. The crystallinity of the PPS found to have effectively increased the conductivity of the TaF_5-doped PPS. However, these studies resulted in conductivities only in the semiconducting region of 10^{-8}-10^{3} S/cm and the use of fluorine-based strong acceptor dopant [5]. Tanabe et al. had discussed the electronic structure of conductively stable SO_3-doped PPS by steady state conduction spectra [78]. The SO_3-doped PPS was found to have conductivity of 2S/cm and mobility of 3.6 cm^2/Vs upon absorption of photo radiation.

Apart from chemical dopant, other studies to improve the electrical conductivity was also investigated. Bratko studied ion irradiation to films of PPS by using ions of lithium, iodine and fluorine to study the effects of its conductivity. While iodine and fluorine ions significantly improve the conductivity, lithium ions were not found to have any substantial affect due to its too low depositions rates [5]. This study had been preceded by Mazurek, where halide ions were used in doping of PPS. In this study, bromine implanted PPS resulted in significant increase of conductivity in the second set of the experiment [79]. It was also suggested that the conductivity of iodine-doped PPS could be stabilized by introducing dyes of violanthrenes, anthraquinones and phthalocyanine to the doped PPS [72]. However, stability issues regarding the iodine-doped PPS is a significant problem. Radhakrishnan suggested that PPS can be doped with $FeCl_3$ and exhibit semiconducting behavior [80, 81]. Although more stable

than other dopants, $FeCl_3$-doped PPS will be limited to semiconducting application due to low conductivity. Rubner also underlined that known dopant of PPS; AsF_5 and SbF_5 have tendency to form charge transfer complex that resulted it to be easily hydrolyzed in contact with water, resulting instability under normal conditions. Thus, they attempted to use nitrosyl salts at 38% mole ratio as potential stable dopant to PPS in nitromethane solution. However, only $NOPF_6$ is relevant to be used but limited to vacuum environment. This is due to rapid decrease of conductivity observed during reaction with water vapor in air [64].

Table 2.5.1 summarized the critical reviews on organic and inorganic dopants while Table 2.5.2 summarized the critical reviews into more recent nanomaterials dopants.

Based on the above research work, it is realized that the mechanism of conductive polymer is due to the disturbance in the polymer chain. In PPS, it is particularly the delocalization of the Π-bond. The delocalization of Π-bond corresponds to the distortion of the polymer chain. For the distortion to happen, dopant must be able to intrigue the double bond characteristic of the C-S bond [5, 69, 82]. The temporary double bond formed between these atoms in the polymer chain will cause disturbance in the readily delocalized Π-electrons of Π-bonds in the phenyl rings of PPS. The disturbance will distort the polymer chain and enhance further delocalization of the Π-electrons in the polymer. The enhanced delocalization promotes electron

mobility and thus expected to increase overall polymer conductivity. Therefore, from this critical review, it appears that the doping of PPS with nanosilver to enhance the conductivity by distortion of the PPS polymer chain is yet to be investigated. Thus, several important parameters for the doping of PPS and nanosilver are therefore yet to be established.

Table 2.5.1: Summary of Critical Review on PPS researches.

Dopant	**Results/Observation**	**References Authors**
Nitrosyl salts up to 38mol%	NOPF6 at 36.3mol% reveals highest conductivity Only NOPF6 relevant to be used and limited to vacuum environment Rapid decrease of conductivity observed due to reaction with water vapor in air.	Michael Rubner et al.
Annealed acceptor-doped PPS	Annealing effects on conductivity of acceptor-doped PPS Unannealed - 0.18 S/cm Annealed - 0.22 S/cm	N. E. Murthy et al.
Organic acceptors (TCNE, TNF, p-chloranil, DDQ)	DDQ and TCNE increased the conductivity of PPS to 10-9 and 10-11 S/cm respectively.	Shizuo Tokito et al.
SO3	Conductivity enhancement are limited.	S. Kazama et al.
SO3	2 S/cm and 3.6 cm2Vs upon absorption of photo radiation	Tanabe et al.

Electrochemical doping in concentrate sulphuric acid	Cyclic voltamertry curves, voltabsorptiometry and electronic spectra	C. Arbizzani et al.
Tantalum Flouride (TaF5)	10-3 to 10-2 S/cm conductivity acheived	Jun Tsukamoto, Seiji Fukuda
Annealed uniaxially and biaxially TaF5	Semiconducting region of 10-8-103 S/cm	Ko et al.
Antimony Pentaflouride (SbF5)	20% PPP – 10 S/cm, in nitrogen atmosphere	D. R. Rueda et al.
FeCl3 in nitromethane	6x10-5 S/cm after 3 hours in 0.1M solution of FeCl3	P. Hruszka et al.
Iodine with CuPH (Copper phthalocyanine)	Marginal conductivity improvement without CuPH With CuPH, lowest resistivity is at 30 mol% at 10-3 S/cm.	Radakrishnan et al.
ASF5	0.01 S/m (maximum) Films produced with ASF3 solution of ASF5-doped PPS - 2 S/m (0.01 – 0.1 S/m)	Shacklette et al.
ASF5	0.01-0.1 S/m, instability in air and upon contact with water	Clarke et al.
Annealed uniaxially and biaxially with TaF5	Semiconducting region of 10-8-103 S/cm	Ko et al.
Iodine, fluorine and lithium	Iodine and fluorine significantly improved the conductivity Lithium ions have no substantial effect due to low depositions rate	Bratko et al.
Halide ions (Bromine)	Significant increase in second set of experiment	Mazurek et al.

FeCl3	Exhibit semiconducting behaviour	Radakrishnan et al.
Iodine (with dyes of violanthrene s, anthraquinones and phthalocyanine)	Stable iodine-doped PPS	

Table 2.5.2: Critical review on PPS doped with nanomaterials and micro-copper

Dopant(s)	**Results/Observation**	**Nanomaterials**	**Author(s)**
Multi-walled carbon nanotubes (MWCNT), Special carbon fibre (SCF) and carbon graphite flakes	• Focus on surface mechanical properties	• MWCNT at 3% • Carbon graphite flakes at 10% • SCF at 15%	Arash Golchin et al.
Carbon fibre reinforced PPS/PTFE	• Surface morphology and mechanical behavior only	• Melt blending at 265-295C	Wei Luo et al.
Nano-diamond	• Nano-diamond as nucleating agent	• PPS:nanodiamond; 100:0 to 97:1 • Melt blending with twin-extruder machine at 220-280C	Shuling Deng et al.

Carbon Nanotubes (CNT)	• Dynamic mechanical and electrical properties • With addition polytherimide and inorganic fluorine-like nanoparticles	• Melt mixing using extruder at 320°C	Diez-Pascual et al.
Nano TiO2-SiO2 into PPS fibers	• No effects on conductivity.		Dandan Lian et al.
Expanded Graphite (EG) and Ultrasonicated Expanded Graphite (S-EG)	• Conductivity with EG – 10^{-2} S/cm. • Conductivity with Ultrasonicated EG – 10^{-3} S/cm.	• Both at 10% graphite compositions.	Y. F. Zhao et al.
Multi-walled Carbon Nanotubes (MWCNT)	• Stages of resistivity drop: 1.Gradual for 0.2 to 5% 2.Sharp decrease 5-7wt% 10^{-12} - 10^{-7} Ohm.cm 3.Limited decrease 7-11wt%	• Range of 0.2 – 11% • Melt blended	Jinghui Yang et al.
Micro particles of copper in ethanol solvent	• The highest conductivity achieved at 60wt% of copper (4.2 x 10-7 S/cm). • Conductivity decreased at 75wt%.	• 0, 30, 45, 60, and 75wt% of copper • Experimental temperature at 100°C.	R. K. Goyal et al.

CHAPTER 3

MATERIALS AND METHODOLOGY

3.1 Overall Methodology

The focus of this research is the doping of nanosilver into PPS. The overall methodology is described in Figure 3.1.2. The preliminary approach was to identify the effective mixing speed for the solid solution of nanosilver and PPS. To determine the effective mixing speed for the doping process, a series of experiments were conducted. The experiments in six different mixing speeds were selected as 60rpm, 80rpm, 100rpm, 120rpm and 140rpm. The surface morphology of the samples was studied using the Optical Micrography and the effective mixing ratio were revealed. Then, the first objective was to identify the effective mixing temperature. The threshold melting temperature was determined as 380℃ after heating the solid solution in different temperatures in the range of 300−400℃. After the threshold temperature was established, the effective melting temperature of the organometallic hybrid was investigated in the range of 400-480°C. The thermal temperature behavior of the

hybrid material investigated under SEM and the most effective temperature was revealed thus Objective 1 was satisfied.

Then, the concentration of nanosilver in PPS was varied and processed with the effective temperature found in Objective 1. The concentrations ranged between 10 to 60% according to the research work conducted by Zhao et al. and Diez-Pascual et al. [51, 74]. The surface morphology and material properties of the samples were analyzed by using SEM and FTIR to study the effective melting temperature and the effect of concentration of the organometallic hybrid, thus Objective 2 was satisfied.

After Objective 2 was achieved, each of the samples were subjected to electrical insulation tester and high voltage conductivity to obtain electrical resistivity of the newly developed organometallic hybrid, thus Objective 3 were satisfied. The results were collected, and conclusion were made based upon the analysis.

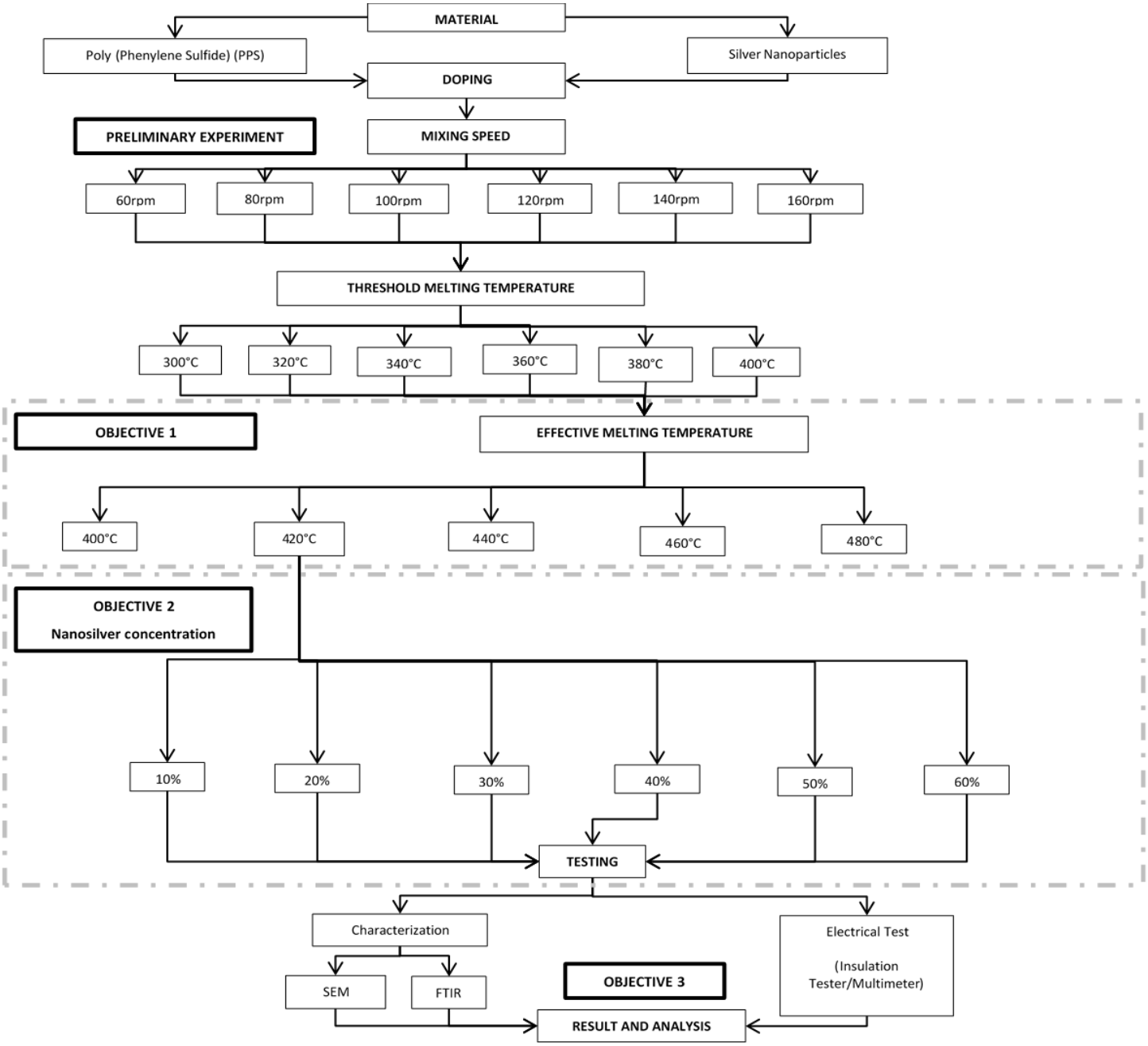

Figure 3.1.1: Overall Experimental Methodology

3.2 Materials

All materials used in this study were supplied by Sigma-Aldrich. The PPS is in powder form of molecular number of approximately 10,000Mn. The nanosilver powders are 99.5% trace metal basis.

3.3 Preliminary Experiments

The preliminary experiment involves two main studies. The mixing ratio between PPS and nanosilver are fixed at 3:1. The first objective is to find the effective mixing speed to mix the PPS powder and nanosilver particles for a homogenous solid solution. The solid solutions were then melted at temperatures varied between 300°C to 400°C at 20°C intervals to determine the threshold melting temperature.

3.3.1 Solid Solution Mixing Speed

The effective mixing speed and mixing time were studied. 1 gram of nanosilver were added into a beaker with 3 grams of PPS powder. The solid solutions were stirred for 15 minutes by 5mm magnetic bar with the speeds varied from 60rpm until 140rpm with 20rpm increment in between. The mixed solutions were then excited at 420°C which was determined during threshold melting temperature investigation and explained in Section 4.2.2. The behavior of the solid solutions after 15 minutes of melting was observed. The samples were then examined under optical microscopy for surface characterization analysis to determine the most effective mixing speed to produce the solid solution.

3.3.2 Threshold Melting Temperature

A range of temperature were investigated to determine the effective threshold temperature for melting the mixture. From the critical reviews, the melting temperature range of pure PPS was between 285°C-295°C [8]. Those experiments however, used PPS in pellet form and employed processes of sintering or melt-mixing using extruder machines which is completely different from the melting by using solid solution. In this study, the PPS powder and nanosilver mix were melted in a beaker. The addition of nanosilver into the PPS polymer matrix affected the melting temperature due to the presence of metal particles which will absorb the heat prior to heat transfer to the polymer according to the first law of thermodynamics.

In this experiment, known PPS melting temperature was used as the starting point for melting process for the solid solutions. The mixture of PPS and nanosilver were pre-mixed by using a magnetic stirrer at 80 rpm, of which was found to be the effective mixing speed of the solution for 15 minutes. After then, the solid solutions were excited in the temperatures ranged from 300-400°C for 15 minutes, three samples from each melting temperatures that were successfully melted were cured at 30°C for 24 hours.

3.4 Structural Properties at Various Melting Point of Nanosilver Doped PPS

The previous study of threshold melting temperature revealed that there is a critical melting temperature for the mixture of PPS and nanosilver. The PPS powder were found to not entirely melted in the typical temperature of 285-295°C [8, 74, 75, 77] due to the existence of nanosilver particles which explained by first law of thermodynamics. Thus, in this experiment, the information obtained from the previous research were used to study the effect of melting temperature to the behavior of nanosilver in PPS. With results of effective mixing speed obtained in 4.2.1, the temperatures ranging from 400 to 480°C with the increment of 20°C in between are used. The samples from the melting process were examined for morphology analysis and electrical behavior test were performed to identify the most effective melting temperature of the organometallic hybrid. The findings were presented and discussed in Section 4.2.3.

With reference to the previous study of effective melting temperature, the effect of concentration of nanosilver in PPS were performed. In this study, the PPS were doped with nanosilver concentrated in the range of 0-60% by weight. The solid solution was prepared by mixing the powders with the effective mixing speed and were melted using the effective melting temperature which was found earlier. The samples were then undergone electrical behavior tests and the morphology studies supported

by SEM and FTIR. The finding of the correlations between electrical behavior to the morphology and FTIR spectra were presented in Section 0.

3.5 Characterization

Each sample produced from the experiment are put unto a sample slide. All samples prepared underwent characterization by optical micrography on preliminary experiments to observe the significant surface morphology. Then, Scanning Electron Microscopy (SEM) of up to 5000X magnification were employed to determine thermal effects of melting temperature and evolution of morphology due to varying concentrations. The evolutions of the morphology for each sample were observed in term of the distribution of the nanosilver and nucleation formation.

FTIR spectroscopy were also done to indicate the change in the molecular structures of the organometallic hybrid especially the C-S bond characteristic. The trend of which the absorption of the infrared across the wavelength in each sample were observed.

3.6 Electrical Behavior Testing

All samples produced underwent electrical behavior testing using insulation tester and high voltage digital multimeter to determine their resistivity. The typical process of taking the resistivity and conductivity measurement by using the equipment strobe are shown in **Error! Reference source not found.**. The value retrieved were t

hen recorded and the resistivity value were obtained from the insulation tester/multimeter.

Figure 3.6.1: Electrical Behavior Test

The test was repeated 3 times for each sample by varying the point of which the test pen is touching the sample. The values obtained on the insulation tester/multimeter are then taken and the conductivity/resistance of the sample are then calculated using the formula shown below:

$$Conductivity, \sigma = \frac{length\ of\ sample\ (l)}{resistivity\ of\ sample\ Ohm\ (r) x\ cross-sectional\ area\ of\ sample\ (78.54 cm^2)}$$

The conductivity values of each sample are then tabulated and standard deviations of the conductivities were calculated.

CHAPTER 4

RESULTS AND DISCUSSION

4.1 General Introduction

This chapter discusses and analyses the results of all experiments conducted in the previous chapter. Effective mixing speed were found by varying mixing speed from 60-140rpm. The threshold melting temperature was determined by melting process in the range of 300-400°C. The effective melting temperatures were observed by melting the solid solution from 400-480°C. Morphology evolutions from these experiments were studied using SEM. The morphology findings were utilized to correlate with the electrical behavior and molecular changes in FTIR spectroscopy. All observations were discussed in the following sections.

4.2 Preliminary Experiments

The effective mixing speed and threshold melting temperature were found during the preliminary experiments. It was revealed that there is an effective mixing speed to produce a homogenous solid solution. The solid solution produced were then used to find the threshold melting temperature of the solid solution which expected to be shifted due to introduction of nanosilver. The results of these preliminary investigations are discussed and presented in the following section.

4.2.1 Solid Solution Mixing Speed

Figure 4.2.1 shows the trend of the distribution and uniformity of the sample surface under 1000X magnification. At 60rpm, the formation and homogeneity of the sample were observed to be non-homogenous as shown in Figure 4.2.1(a). There were two large bright spots in a dark ring as nanosilver which surrounded the compacted PPS powders. The non-homogeneity was due to the amount of kinetic energy supplied to the solid solution. At 60rpm, the kinetic energy supplied is not enough to diffuse the powders together and caused the materials to be kept segregated. Further increase of the mixing speed at 80rpm, the surface observed to be more evenly distributed and homogenous throughout as shown in Figure 4.2.1(b). Similar result could also be seen on sample mixed with 100rpm mixing speed.

At 120rpm, the surface formation shows the surface becoming less homogenous again. There are some distinct bright spots at which the polymer powder was found compacted. Nevertheless, no big dark areas of nanosilver i.e. dark ring were found which indicates it was dispersed throughout the solid solution except for the compacted PPS. At 140rpm, the large bright spots became as large as in 60rpm. This indicated that the homogeneity is becoming even less as mixing speed increased above 100rpm. This showed that the higher mixing speeds of 120rpm and 140rpm deemed not effective to produce homogenous organometallic hybrid. The energy supplied was found to be in excess and caused the components to be compacted by the centrifugal movement of the magnetic stir bar. The compacting of the PPS powder was hindering further diffusion of nanosilver into PPS similar to study made of mechanical mixing of polythiophene with nano copper [83].

As a conclusion, the effective mixing speed of the solid solution of nanosilver doped PPS is between 80rpm and 100rpm. At these two speeds, the samples appeared to have homogeneity as per microscopy images. Therefore, the effective mixing speeds to dope the nanosilver into PPS is identified between 80rpm and 100rpm. Nevertheless, 80rpm was chosen as the effective mixing speed in this investigation.

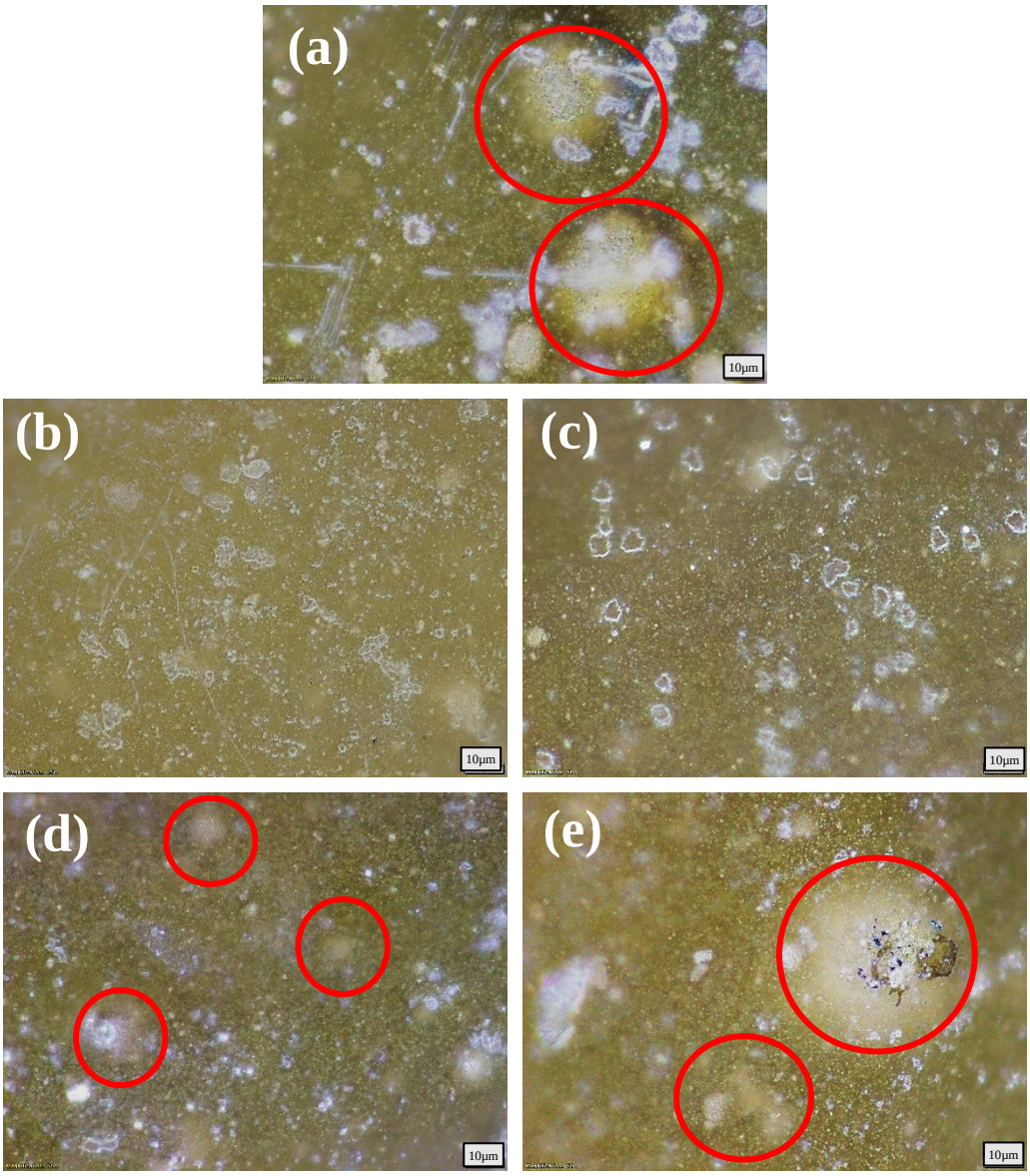

Figure 4.2.1: Micrography images of variable mixing speed of solid solution for nanosilver doped PPS; (a) 60rpm, (b) 80rpm, (c) 100rpm, (d) 120rpm and (e) 140rpm.

4.2.2 Threshold Melting Temperature

Table 4.2.1 summarizes the melting start time of the mixture and thorough melting of the solution. In the temperatures from 300°C to 360°C, it was observed that the solid solution had not melted completely within the 15 minutes period. In other words, at these temperatures the heat supplied were insufficient to excite the entire mixture. The mixture had not absorbed enough heat energy from the source to increase their overall temperature sufficient for melting and triggers diffusion. When the temperatures were increased to 380°C and 400°C, complete melting of the solid solution happened. The time taken when the mixture started to melt were found to be dropped significantly to below 8 minutes when the melting temperature were increased from 380°C. It is assumed that there is sufficient heat absorbed by the nanosilver for the continuous heat supplied to be melt the polymer. The typical sample of incomplete and completed melting of the solid solution are shown in Figure 4.2.2.

Table 4.2.1: Mixture Melting Temperature Experiment Observation

Temperature, °C	Melting Start Time, minutes	Observation
300	N/A	Incomplete melting
320	35.0	Incomplete melting
340	20.0	Incomplete melting
360	16.0	Partial melting after 15 minutes
380	7.5	Thorough melting after 15 minutes
400	6.2	Thorough melting after 15 minutes

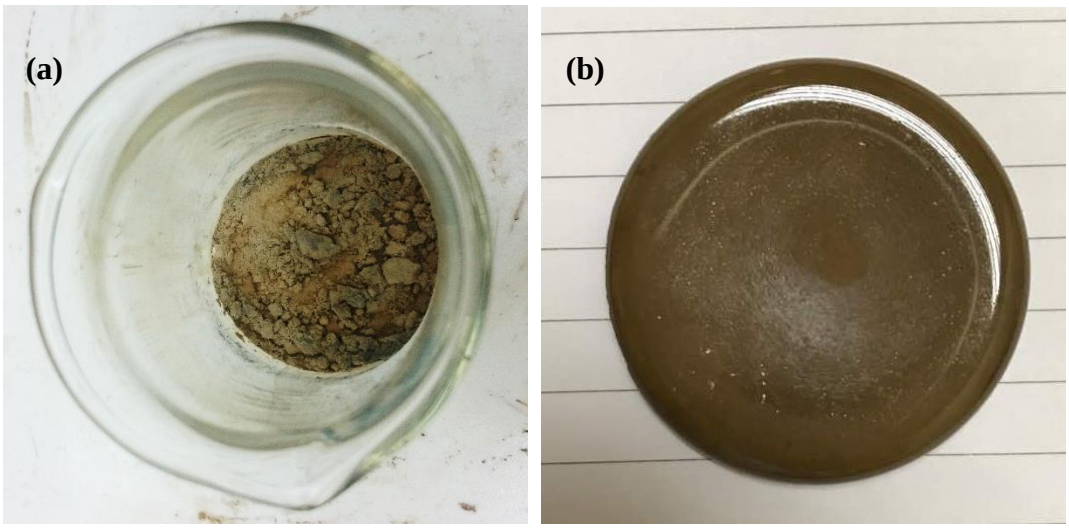

Figure 4.2.2 (a) The typical conditions of incomplete melting of solid solution below the threshold temperature (b) The complete organometal hybrid melted above threshold temperature of 380°C

The organometallic hybrid observed to have completely melted at 380°C above (400°C) within 15 minutes. This indicates that the threshold temperature for melting the solid solution is 380°C. This temperature is significantly higher than the typical melting temperature of solid PPS found in the literatures of around 280-290°C [8, 45,

77, 84]. This threshold temperature for melting led the process of finding the correlation of thermal effect to the effective melting temperature of the mixture.

The relation between the complete melting time and melting temperature are shown in Figure 4.2.3. The complete melting time had a significant behavior change from 300°C to 380°C. It is observed that the most significant drop occurred between 320°C to 340°C. From temperatures 340°C to 380°C, the time taken to melt were stabilized afterwards at around 6 minutes.

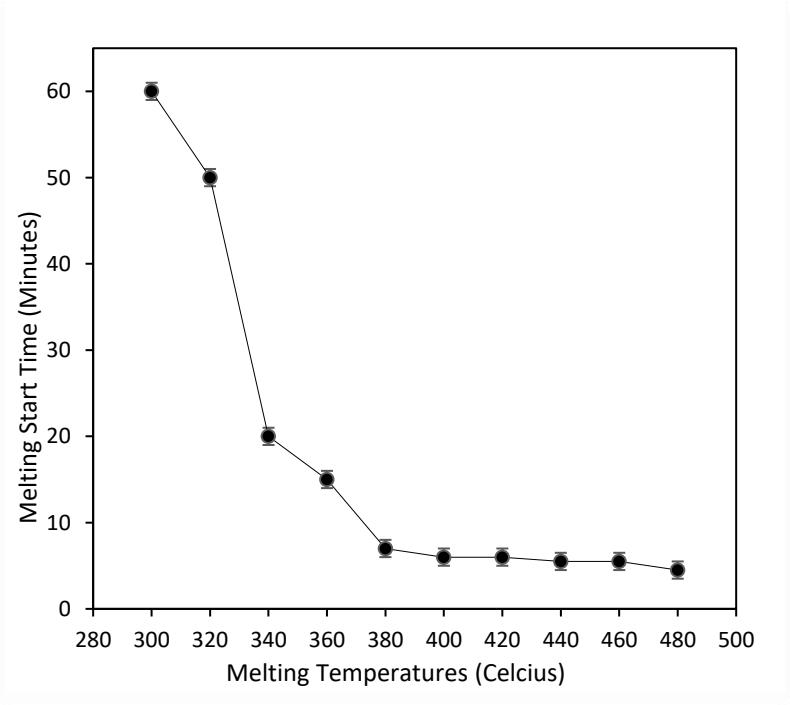

Figure 4.2.3: Graph of Melting Temperature vs Melting Start Time. Melting start time reduced significantly at 340ºC and stabilized at 380ºC to 480ºC.

The phenomenon is best explained by thermal behaviour of most nano particles, which found to be very effective in heat absorption as also utilized by the

studies. In the researches, the addition of nano particles increased the heat absorption rates of nanofluids [85-87]. The behavior is explained by the first law of thermodynamics according to Clausius statement as follows:

$$dQ = dU + dW \text{ [88]}$$

In relation to this research, *dQ* is the energy supplied, and *dU* is the change of internal energy and *dW* is the external work done in the heated system. Change of internal energy *dU* would occur through the absorbance of the heat required to completely breakdown the intermolecular bond which exists between the polymer chains i.e. cause the melting and *dW* is the external work done through exciting the nanosilver for it to diffuse into the polymer matrix. Hence, the heat supplied was not sufficient to melt the solid solution and excite the nanosilver to promote diffusion of both materials to form a hybrid [9]. This explain the observed shifting behavior of melting point of the nanosilver doped PPS hybrid.

4.2.3 Structural Properties at Various Melting Point of Nanosilver Doped PPS

Thermal behavior of the organometallic was studied in the range of temperature of 400-480°C. The samples were labeled as such; ST400 is for sample melted at 400°C, ST420 for 420°C and such. The trend in nucleation formation was observed. In Figure 4.2.4, the images of ST400 displays the significant surface

roughness where there are bright masses visible across the sample. These are non-uniformly distributed non-melting PPS coagulations due to insufficient heat supplied and high heat absorption by the nanosilver as discussed in 4.2.1. However, in this case, the coagulations are much smaller and could only be seen under SEM microscopy.

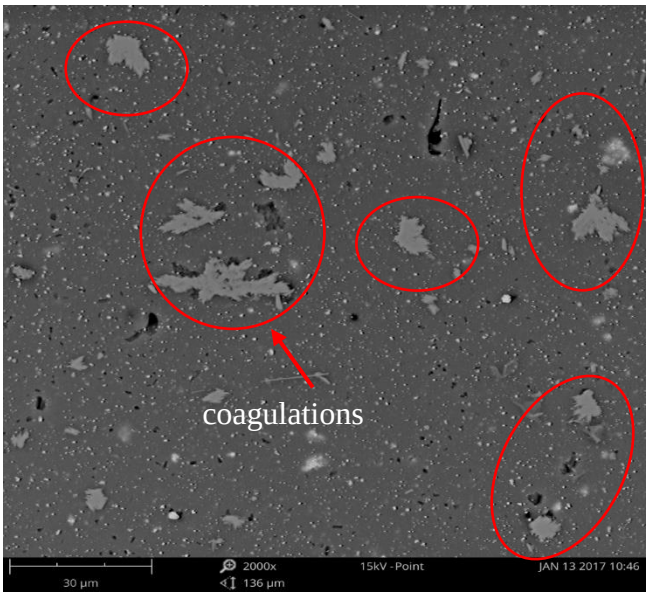

Figure 4.2.4: SEM Image of ST400. Some coagulations can be found (red circles) indicating incomplete melting of the PPS at 400ºC.

The morphology was found to be the most even at 420°C. As observed on the sample ST420 in Figure 4.2.5, less localized and smaller bright spots are visible. It is observed to having almost no porosity compared to other samples, proving that minimum gases are trapped indicating minimum amount were produced at this temperature. This shows that at this temperature, enough heat energy was supplied and absorbed throughout the solid solution. This sufficient energy supplied assisted in the

production of homogenous diffusion of nanosilver prior to dehydrogenation of PPS. Apart from homogeneity, nucleation were also observed in this sample.

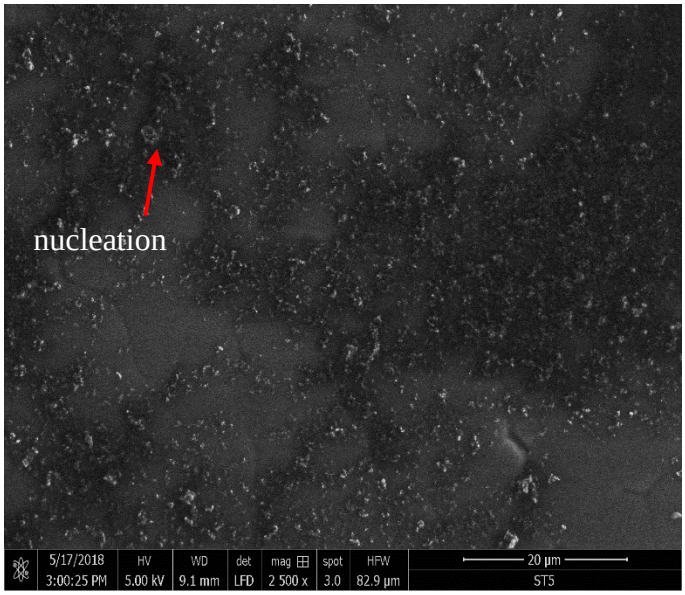

Figure 4.2.5: SEM image of ST420. Arrow shows nucleation of which starting to form at this melting temperature of 420ºC.

However, significant changes of morphology behavior happened around 440-480°C. In Figure 4.2.6, contrasting bright spots can be seen dispersed throughout the sample's scanned area. As the temperature increased from 440°C to 480°C, the populations of the bright spots were also appeared to be increased. In these temperatures, it is known that PPS undergone primary decomposition process into several cyclic oligomers. It is observed that the porosity on these samples are becoming more obvious as the temperature raised. The voids might be caused by the by-products of dehydrogenation in the higher decomposition temperature of PPS [89]. It is important to note that, at these temperatures, significant fumes were released during

melting process of the solid solution as more gases such as hydrogen sulfide, hydrogen, methane and benzene released [45, 46, 90]. Thus, the higher the melting temperature, the higher level of porosities are found.

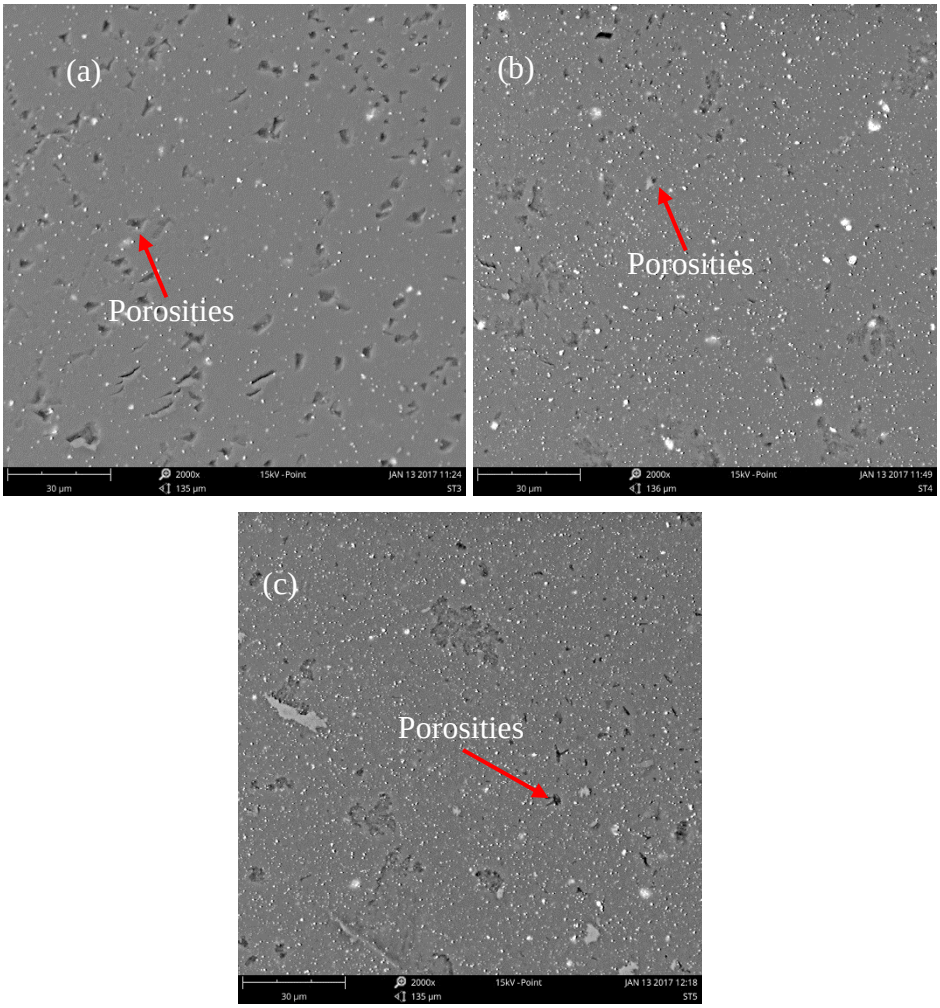

Figure 4.2.6: SEM images of (a) ST440, (b) ST460 and (c) ST480. Arrows shows the porosities that formed through this temperature range (440-480ºC).

4.2.4 Electrical Behavior

Figure 4.2.7 shows the result of the resistivity of the organometallic hybrid against the melting temperature. It is observed that all sample exhibit resistivity of pure PPS at $1.6x10^{-16}$ Ω.cm. In other word, the variation of melting temperature has no significant effect on electrical behavior of nanosilver doped PPS. This is due to the fact that at these energy level, such diffusions of nanosilver were not sufficient to initiate adequate delocalization of electrons.

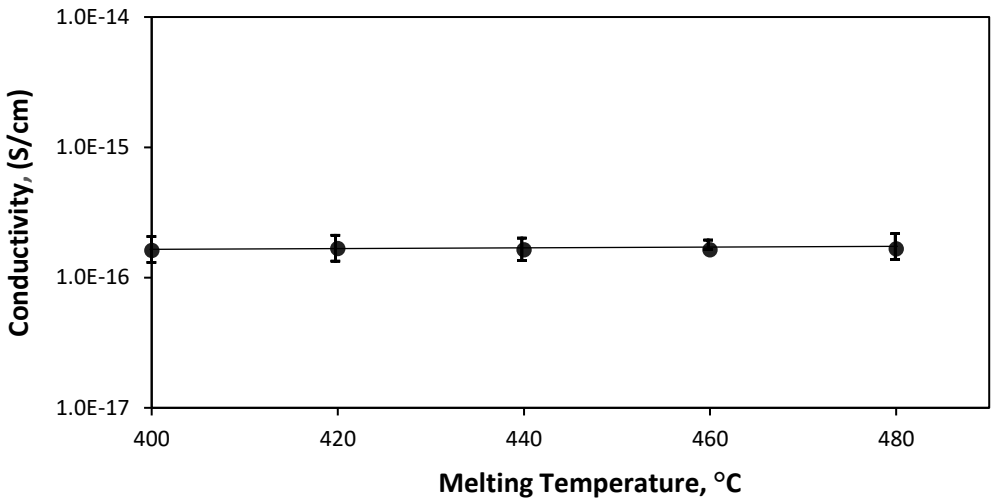

Figure 4.2.7: Electrical conductivity of nanosilver doped PPS as a function of melting temperature.

4.3 Influence of Doping Concentration on Nanosilver Doped PPS

In this section, the influence of concentration on the electrical behavior as well as morphology of the organometal were studied and the coherence between the two are explained. Furthermore, the FTIR spectra were explained which are in good agreement with both findings.

4.3.1 Morphology

In this section, the morphology of the organometal hybrids with different concentrations of nanosilver were discussed. Interesting formation of cluster and nucleation of silver particles were observed as the concentrations were increased. The progressive development of the nucleation are described in details.

In Figure 4.3.1, pure PPS morphology is shown. In this image, it is clearly exhibited that there are no bright spots of nanosilver found. In addition to the absent of bright spots, it is seen as smooth. This pure PPS morphology is taken as a benchmark on how the morphology transformed over the increment of nanosilver concentrations.

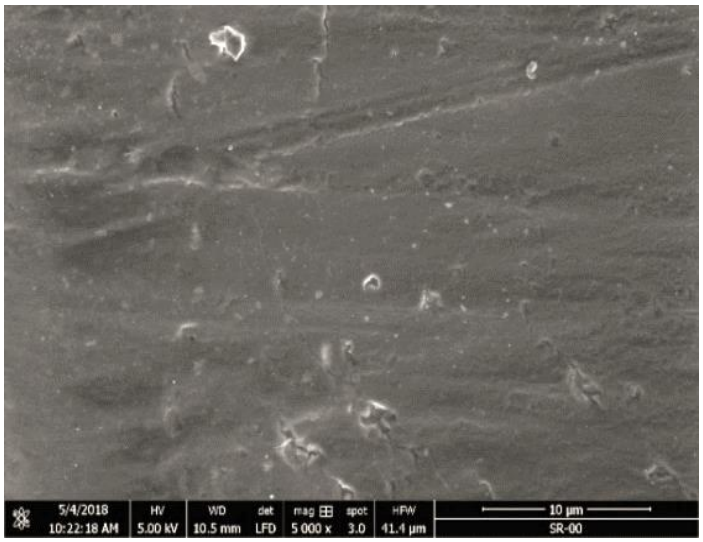

Figure 4.3.1: Morphology of pure PPS (SR-0). Smooth surface shows no trace of nanosilver.

Meanwhile, as the nanosilver added into the PPS matrix by 10% concentration, the existence of nanosilver particles are observed in Figure 4.3.2. Very limited bright spots could be clearly visible throughout the scanned area. These bright spots are nanosilver inside the polymer matrix of PPS. The bright spots are dismal in size and there is no apparent nucleation could be identified.

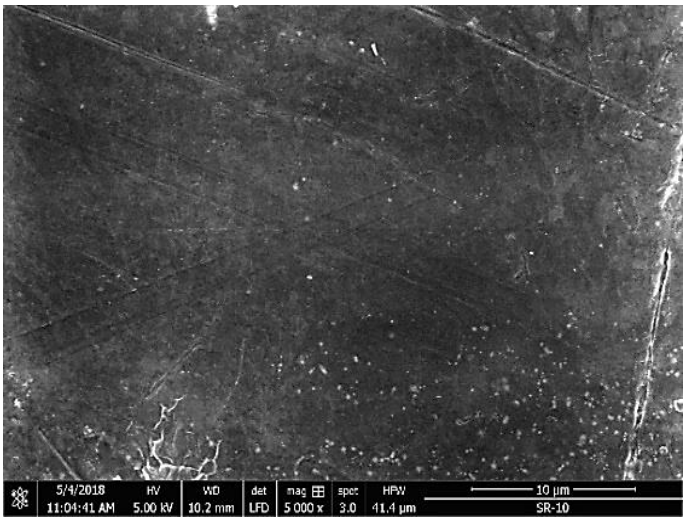

Figure 4.3.2: Image of SR-10 of PPS with 10% nanosilver content. Dismal sized bright spots without apparent nucleation could be identified.

The bright spots are becoming obvious as the concentration increased to 20%. In Figure 4.3.3, the nanosilver are observed to be well dispersed across the image. The nanosilver were found to be larger in size in comparison of spots in SR-10 which is becoming apparent as the nanosilver are starting for form clusters of larger sizes.

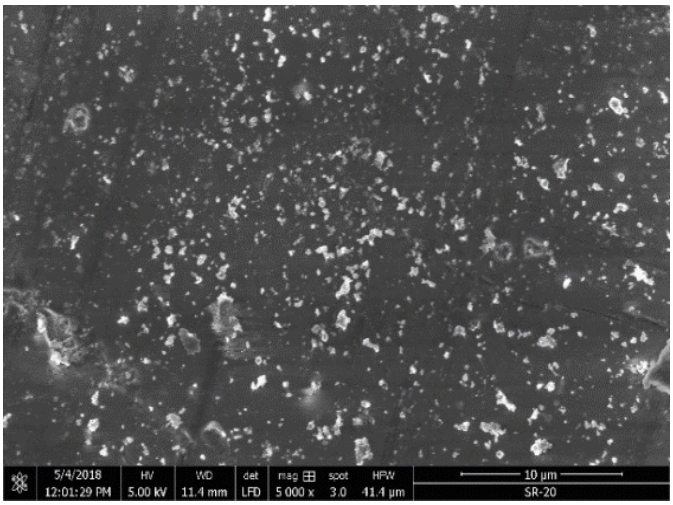

Figure 4.3.3: Image of SR-10 of PPS with 20% nanosilver content. Obvious bright spots of the nanosilver in clusters are observed.

The formation of cluster progressed as concentration is further increased to 30% as observed in Figure 4.3.4. The nanosilvers formed clusters that grown even larger and localized in groups of clusters. However, the clusters are still found to be indistinct and dispersed throughout. The nucleation are similar to SR-20.

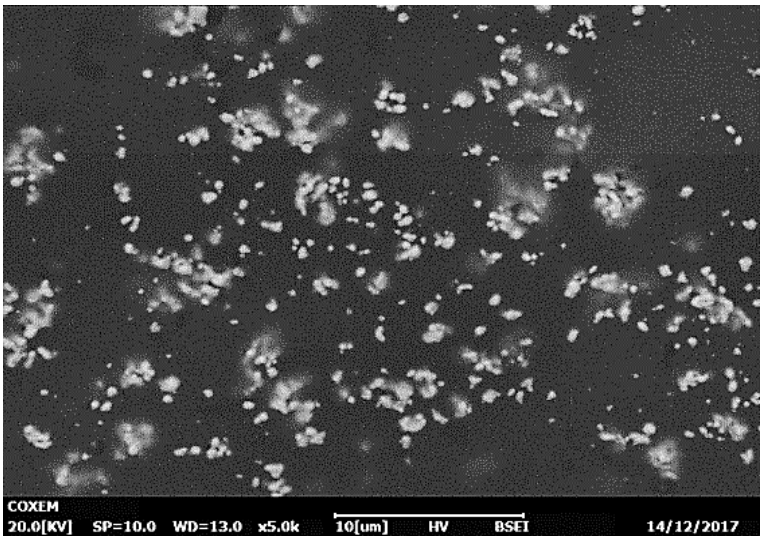

Figure 4.3.4: Image of SR-30 of PPS with 30% nanosilver content. Larger localized clusters of nanosilver are observed.

The morphology progressed rapidly with the increment of another 10% of nanosilver content in SR-40 as observed in Figure 4.3.5. The organometal underwent very distinct nucleation formations which the borders of the clusters could be observed unlike in the hybrids below 30%. The nucleation also spread widely across the polymer matrix. It is recognized to be very discreet in comparison of the organometals from 30% concentration and below.

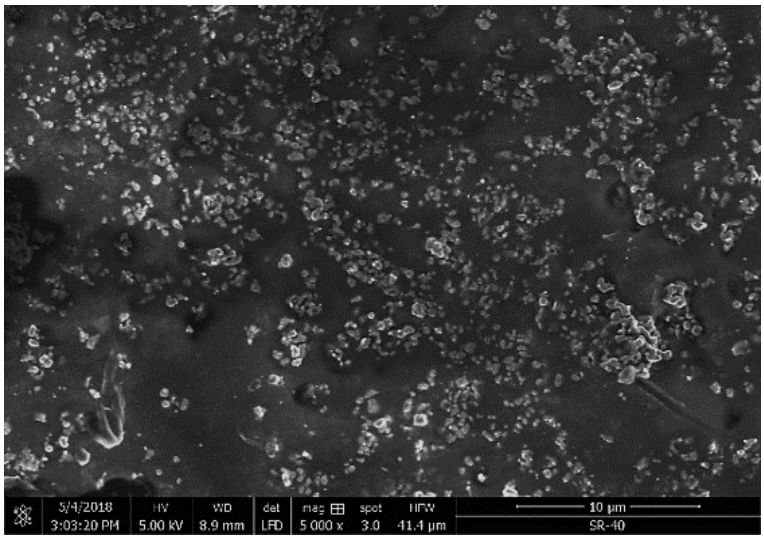

Figure 4.3.5: Image of SR-40 of PPS with 40% nanosilver content. Very distinct nucleation formations which the borders of the clusters could be observed unlike in the hybrids below 30%.

The nucleation further progressed in SR-50 as shown in Figure 4.3.6. The morphology presumed to have reached a well-established level as the nanosilver are observed. The nucleation are clearly seen as massive and beginning to saturate.

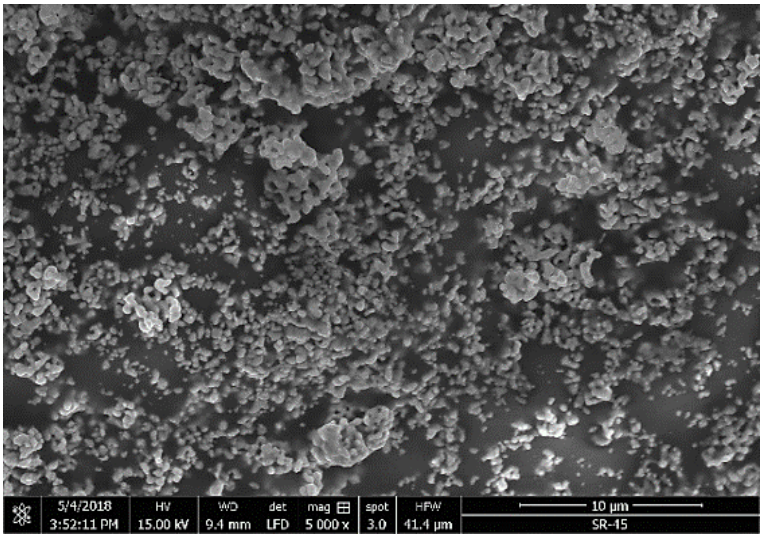

Figure 4.3.6: Image of SR-50 of PPS with 50% nanosilver content. Well-established nucleations clearly seen as indication of saturation.

As expected from the observation in SR-50, the SR-60 clearly seen to have reached a saturation state as exhibited in Figure 4.3.7. The nucleation is seen as combined and the nanosilver dominated the hybrid material. This happened as there is no longer space in the polymer matrix to occupy the nanosilver particles resulting in the accumulations accrued outside the polymer matrix.

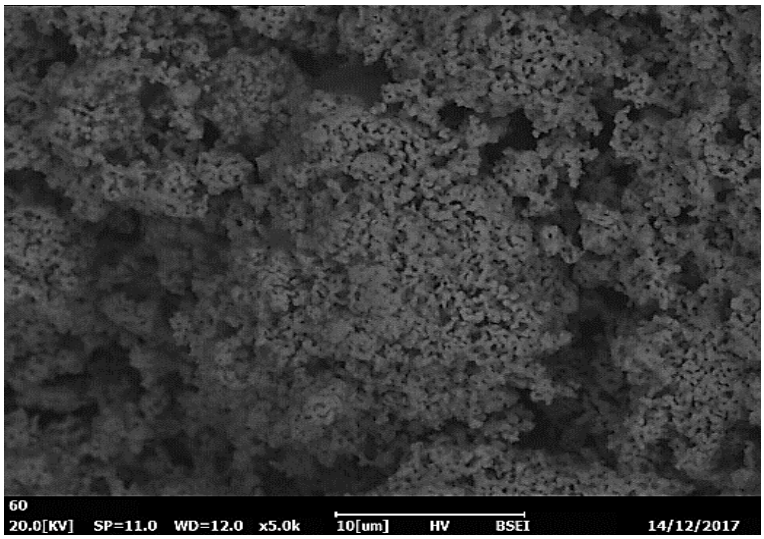

Figure 4.3.7: Image of SR-60 of PPS with 60% nanosilver content. Surface are dominated by combined nucleation of nanosilver.

Figure 4.3.8 summarizes the significant changes of the overall matrix morphology due to variation of the nanosilver concentration. As the concentration varied from 0-30% (Figure 4.3.8a-1d), distinct bright nucleation of nanosilver was formed progressively with the increase of concentrations. Further increased to 40%, it was clearly observed a rapid morphological change of nucleation compared to 30% and below. In this case (Figure 4.3.8e), nanosilver particles tend to form discrete small clusters rather than aggregates as a network of metal particles in polymer matrix. Such

behavior is entirely different as observed in micro-copper network of PPS polymer matrix[8]. As more silver nanoparticles incorporated into the matrix, it facilitated more contact of silver to the atoms in polymer chain especially with sulphur atom in C-S chain of the polymer. Moreover, the enhanced proximities of the nanosilver intrigues silver atoms to Π-bonding of phenyl rings. Such behavior initiates the electron delocalization through the distortion in PPS chain and form the sulfur cation i.e. increase the C-S double bond characteristics [69]. Further increased to 50% of nanosilver (Figure 4.3.8f), the morphology of well-established clusters of nanosilver is evident as it reached to a matured state. In contrast, the overall morphology became saturated at 60% concentration (Figure 4.3.8g).

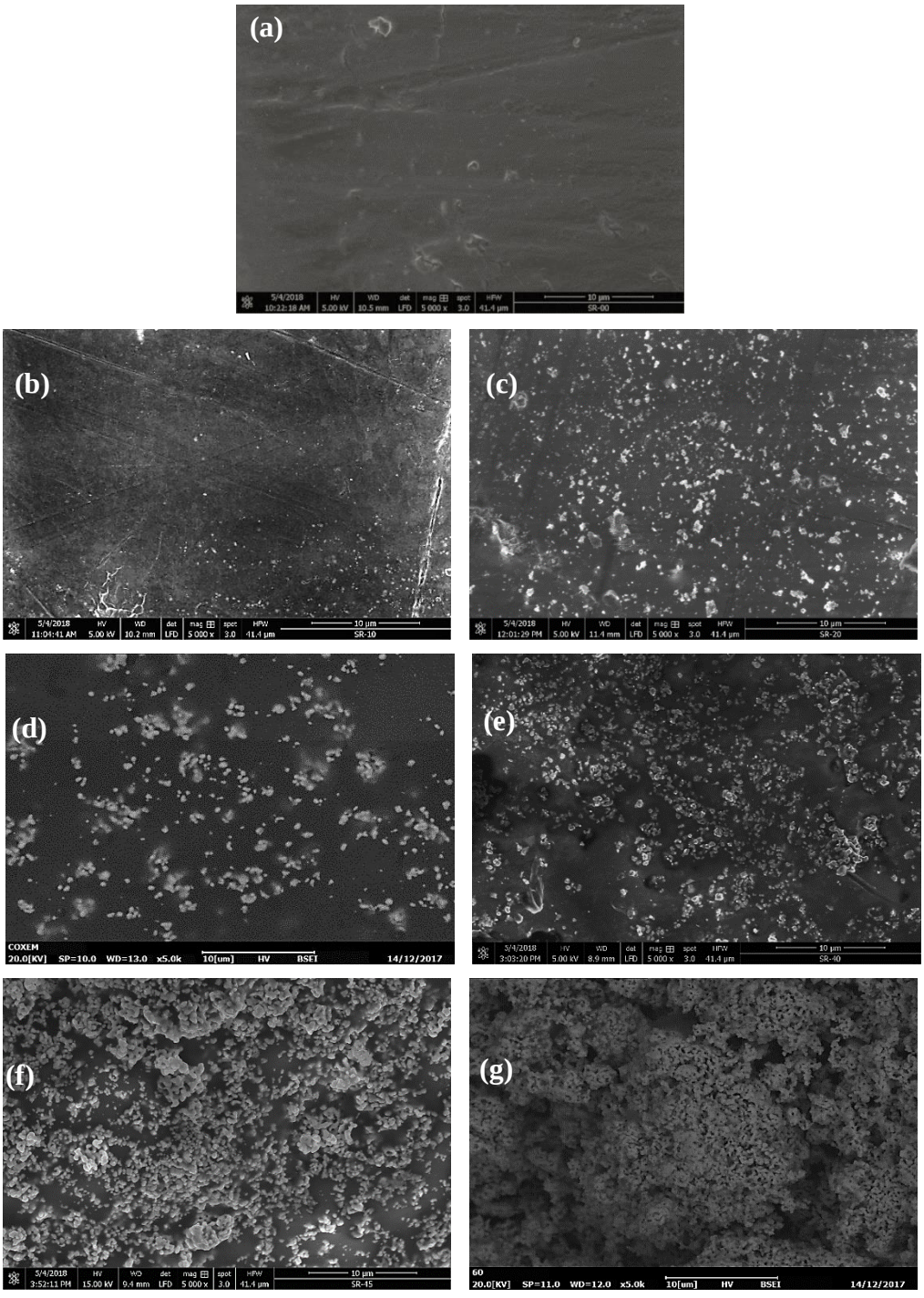

Figure 4.3.8: The summary of SEM images of samples (a) SR-0, (b) SR-10, (c) SR-20, (d) SR-30, (e) SR-40, (f) SR-50 and (g) SR-60. Nucleation are formed progressively in size from 30-50% until saturation at 60% of nanosilver.

4.3.2 Electrical Behavior

Table 4.3.1 and Figure 4.3.9 shows the correlation of the resistivity of the compounds with concentrations of nanosilver. It reveals that from 0-30% of nanosilver particles in PPS, there is no change in conductivity from the pristine PPS. This indicates that there is insufficient amount of nanosilver to intrigue successive phenyl rings in pristine PPS C-S-C plane [5, 69]. Hence, at this stage, doped polymer act as an insulator due to obstructed Π-electrons delocalization in polymer. However, increasing the concentration to 40wt%, the conductivity raised significantly higher to around $1.0x10^{-02}$ S/cm. This conductivity value is only slightly lower than doping of PPS with AsF_5 and TaF_5. Nevertheless, it is higher than silicone and surpassed the conductivity of micro-copper doped PPS at $4.2x10^{-7}$ S/cm [8]. In contrary to the study, in Figure 4.3.8e, it is clearly shown that the structure of the organometallic hybrid has distinct clusters formation. The conductivity has been achieved by massive electrons excitation enhancement in the doped polymer. This is due to the enhanced delocalization of the Π-electrons in the phenyl rings in nanosilver doped PPS polymer [5]. At this concentration, there is sufficient silver in the polymer matrix to disrupt the Π-electrons and distort the PPS polymer chain and increase the C-S double bond characteristic as suggested by the study of conductivity mechanism in PPS [69]. Hence, the C-S bonds in the polymer tend to form the sulfur cation. Thus, the overlaps

of orbitals in the hybrid material were enhanced and provide higher mobility to the electron between the polymer matrix.

Further increase the concentration to 50%, the conductivity only raised marginally to about $1.0x10^{01}$ S/cm which is only around one-fold improvement from the value in 40%. This is due to the maturing of the doped polymer proven by the well-established morphology in Figure 4.3.8e. At this level, there is only limited space left for nanosilver to fill in the polymer matrix to interface with sulphur atoms and disrupt the Π-electrons. At 60% concentration, the conductivity is seen as plateauing at around $1.5x10^{01}$ S/cm due to the saturation of the nanosilver as seen in Figure 4.3.8g. Nevertheless, this is remarkably close to germanium and graphene values [91]. The nanosilver becoming more saturated in the polymer hence limiting further conductivity increase.

Table 4.3.1: Concentration vs Mean Conductivity/Resistance Values

Concentration	Test 1	Test 2	Test 3	Insulation/ Conductivity	Mean	Standard Deviation
10	$1.10x10^{-16}$	$1.00X10^{-16}$	$1.80x10^{-16}$	$1.00x10^{-16}$	$1.00x10^{-16}$	$4.36x10^{-17}$
20	$1.80x10^{-16}$	$9.00x10^{-17}$	$2.00x10^{-15}$	$1.00x10^{-16}$	$9.00x10^{-17}$	$1.08x10^{-15}$
30	$4.80x10^{-10}$	$6.00x10^{-10}$	$5.00x10^{-10}$	$5.00x10^{-10}$	$4.80x10^{-10}$	$6.43x10^{-11}$
40	$2.09x10^{-02}$	$2.19x10^{-02}$	$2.34x10^{-02}$	$2.19x10^{-02}$	$2.09x10^{-02}$	0.001258
50	$3.46x10^{-01}$	$3.28x10^{-01}$	$3.26x10^{-01}$	$3.26x10^{-01}$	$3.26x10^{-01}$	0.011015
60	2.23	2.27	2.24	2.27	2.23	0.020817

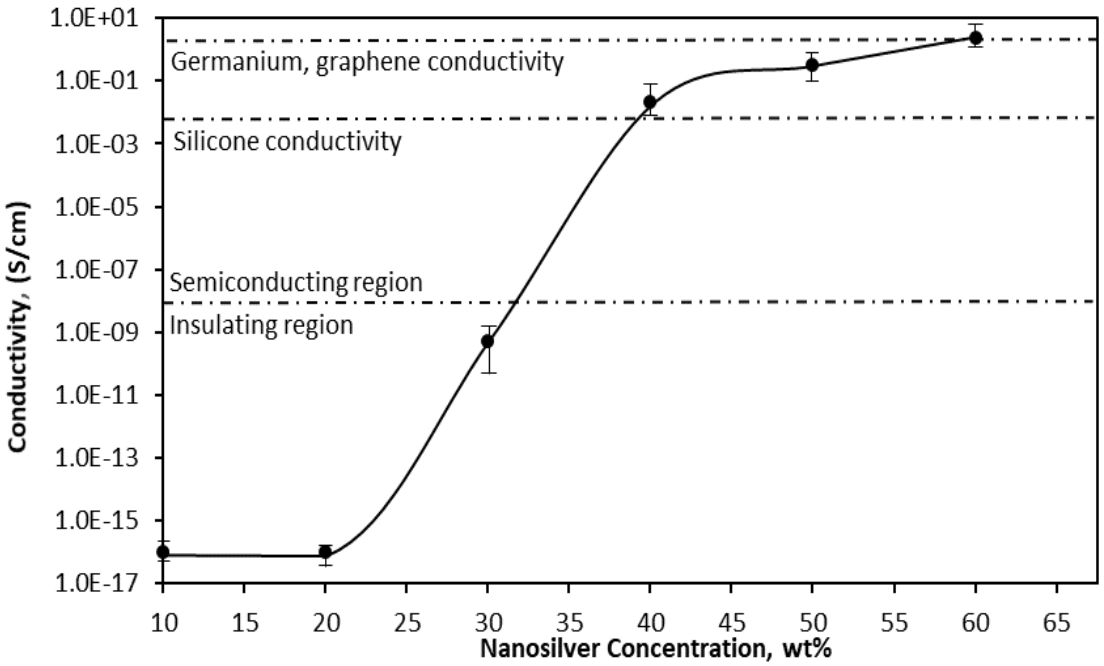

Figure 4.3.9: Electrical conductivity of nanosilver doped PPS as a function of nanosilver concentrations.

4.3.3 FTIR Spectra Analysis

In Figure 4.3.10, the FTIR spectra for nanosilver doped PPS in various concentration are presented. It is interesting to note that there is a distinct characteristic change as the concentrations of the nanosilver in PPS are increased. As shown in Figure 4.3.10(a), the pristine PPS spectra shows a very flat and horizontal trend as the wavelength decreases from 4000nm to 700nm. As the concentration of the nanosilver increased, so does the absorption rate of the infrared that has been clearly noticed by increase of deviation along the wavelength, thus the spectra curved upwards more. This is the same as shown by Tsukamoto et al. in the study of conductivity mechanism of PPS. In that study, it is shown that, as the dopant introduced in the PPS matrix, the spectra absorption level across the infrared spectrum was increased. The spectra absorption rate curved upward as the wavelength decreased as shown in Figure 4.3.11 [69].

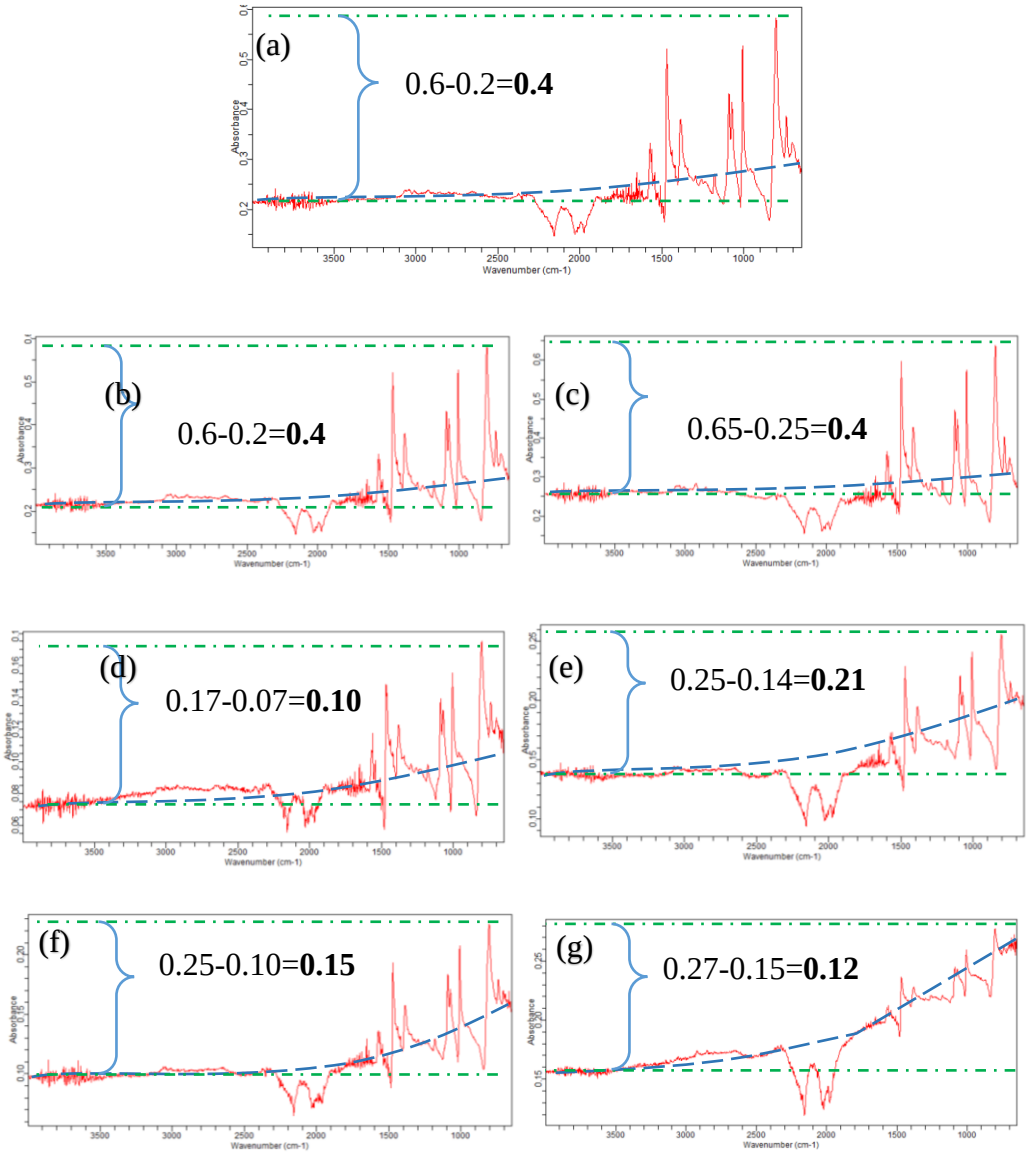

Figure 4.3.10: FTIR Spectra of nanosilver-PPS hybrids in various concentrations. Blue dashed lines show the trend of the FTIR absorption rate as the infrared wavelength reduced from 4000nm to 700nm.

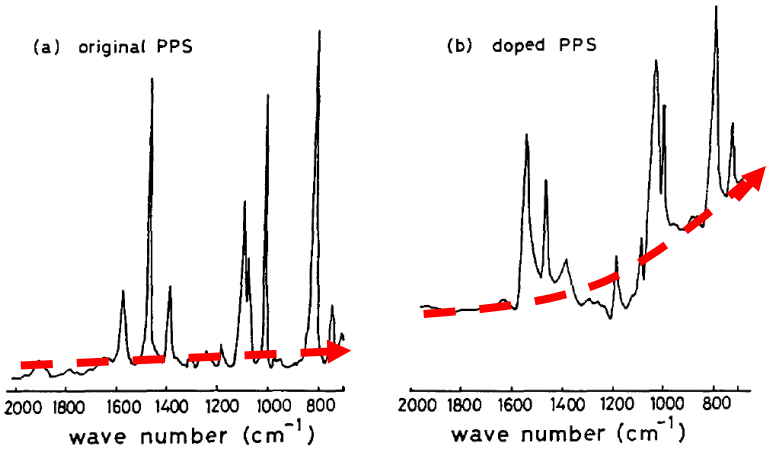

Figure 4.3.11: The FTIR spectra of pure vs doped PPS [69]

To further analyses the FTIR spectra of doped PPS, it is important to understand the philosophy of FTIR absorption by molecules. Electrons in organic molecules like PPS polymer could be in a strong σ-bond, weak Π-bond or non-bonding (denotes by n). These electrons in σ and Π-bond, could be excited and elevated to anti-bonding states, denoted by σ* and Π*. These antibonding states correspond to certain well-defined wavelengths in the spectra. In PPS, C-S bond of which has σ-bond and could be enhanced by having double bond with introduction of Π-bond in the polymer chain play an important role in their conductivity mechanism. This C-S bond corresponds to the wavelength in 1200-1000cm^{-1} and 700-500 cm^{-1}, thus explained upwards curving of the spectra across the wavelength [69]. In interpreting the FTIR of doped PPS, observation need to be the valued between the moiety (two extremes) of the spectra. In this case, the differences of absorption rate at 4000nm to the highest peak seen on each spectrum. For example, in Figure 4.3.10a and Figure 4.3.10b, the

difference between the absorbance value at 4000nm and the highest peak at around 800nm are around 0.4. In Figure 4.3.10d until Figure 4.3.10g, shows the absorbance decreases in the range of 0.1-0.2 and stabilized. This absorbance value corresponds well to the threshold of conductivity. This finding is in very good agreement with the stabilization of conductivity found in electrical behavior test. In other word, both FTIR absorbance and electrical conductivity are very coherent with each other. Both characteristics were coherent to the morphology shown in Figure 22.

In this section, PPS was doped with nanosilver at various concentrations and their influences on the electrical behavior of the organometallic hybrid were investigated. It is revealed that there is threshold concentration of nanosilver which initiates the delocalization of Π-bonding in the phenylene ring of PPS chain. It is also observed that at 40wt% concentration, electron delocalization is triggered through the distortion in PPS chain and form the sulfur cation i.e. increase the C-S double bond characteristics. Hence, massive charge mobility observed as the electric conductivity reached metalloids level at around $1.0x10^{-02}$ S/cm and at 50% concentration, such clusters becomes well-developed and the conductivity plateauing at around $1.5x10^{01}$ S/cm. However, above 50% concentration, the organometallic hybrid reached to saturated conductive state whereas on the contrary, below 30%, this appeared as insulated state.

CHAPTER 5

CONCLUSION

5.1 General Conclusion

In this research, the PPS polymer had been doped with nanosilver to produce electrically conductive organometallic hybrid. It is hypothesized that the nanosilver could increase the conductivity of pure PPS polymer by distortion in the polymer chain particularly by increasing the double bond characteristic in the C-S connection. The distortion would enhance the delocalization of Π-bond electrons. The delocalization of Π-bond electrons are expected to form complex orbitals in the organometallic hybrid, in which will increase high charge mobility. High charge mobility is crucial to produce a high conductive polymer for high voltage application.

To achieve this, various parameters such as effective mixing speed of solid solution, threshold melting temperature and effective melting temperature had been studied. Finally, the investigation revealed that the influence of nanosilver

concentration plays the dominant role in the electrical conductivity change or the organometal. This research also concluded that there is a threshold concentration at which the conductivity of hybrid increased significantly resulted in enhancement of electrical conductivity up to germanium metalloid level which was explained by morphology and FTIR analysis.

The effective mixing speed of nanosilver-PPS solid solution was found by varying the speed of the stir bar in the range of 60-140rpm. Observation with optical microscopy revealed that at 60rpm, the mixing speed was insufficient to produce a homogenous organometal after melting process. Furthermore, higher mixing speeds of over 100rpm was also found to be ineffective as the resulting hybrid material uniformity had not been achieved. It was the mixing speed in the range of 80-100rpm that produce the most homogenous organometal.

The objective to find the threshold melting temperature of the solid solution was performed in the temperatures of 300-400°C. By observing the completeness of the melting process against the melting time of the solid solution, it is found that the melting point significantly increased to 380°C as compared to the range of 285-295°C for pure PPS. This finding has led to the research of the effective melting temperature.

The second objective to find the effective melting temperature of the solid solution in the range of 400-480°C. It was observed that at 420°C, apart from the

minimal porosity, the nucleation of nanosilver particles appeared. Whereas, the temperature of 400°C provide insufficient heat energy and the temperature beyond 440°C led to significant porosities and no nucleation was apparent. Nevertheless, the experiment had not indicated any changes in the electrical behavior due to the insufficient Π-electron delocalization of the C-S bond in polymer chain.

Lastly, the study of the concentration influence on nanosilver doped PPS produced very interesting results. It was observed that there is a threshold concentration which was found to significantly change the electrical behavior of the hybrid material. 40% of nanosilver allows sufficient Π-electron delocalization that distorts the C-S bond in the polymer chain and thus increase the overall nanosilver doped PPS conductivity. The morphology also revealed that the nanosilver nucleation formation had an apparent effect to the electrical behavior of the organometallic hybrid. The electrical behavior was reflected in FTIR study, which showed that as nanosilver dopant progressively increased to 40%, the FTIR absorbance between the nominal level and the peak level significantly reduced. The FTIR spectrum also significantly curved upwards across the wavelength as the concentration increased indicating improved C-S bond characteristics in the polymer.

5.2 Specific Conclusion

A few significant parameters had been established in this study. The effective mixing speed, a threshold melting temperature and effective melting temperature had been found. A coherent relationship between nanosilver concentration to the electrical behavior, nanosilver nucleation and FTIR spectra was also observed. In short, the study had contributed to the establishment of the following:

1. The effective mixing speed for solid solution is 80rpm.
2. More significant amount of heat is required to melt the solid solution due to the addition of nanosilver particles thus reveals the mixture threshold melting temperature as 380°C.
3. The effective melting temperature to obtain nanosilver nucleation was revealed at 420°C.
4. The threshold doping concentration was revealed at 40% which increased the electrical conductivity to $1.5x10^{-01}$ S/cm reaching germanium (metalloid) level.

5.3 Future Work

The doping of nanosilver with PPS should be investigated further. The following are future works to further expand the research regarding nanosilver doped PPS, which are:

1. To study moldability to produce large enough sample.

2. To investigate the use of different mold materials rather than glass such as metal and ceramic.
3. To perform Mechanical properties study of doped polymer.

5.4 References

1. E. R. Fitzharris, N. Watanabe, D. W. Rosen, and M. L. Shofner, *Effects of material properties on warpage in fused deposition modeling parts.* The International Journal of Advanced Manufacturing Technology, 2018. 95(5): p. 2059-2070.

2. H. W. Hill and D. G. Brady, *Poly(arylene sulfide)s*, in *Encyclopedia of Polymer Science and Technology*,(John Wiley & Sons, Inc. 2002.

3. P. Chandrasekhar, *Introducing Conducting Polymers (CPs)*, in *Conducting Polymers, Fundamentals and Applications: Including Carbon Nanotubes and Graphene*,(Cham: Springer International Publishing. 2018). p. 159-174.

4. H. Kaneko, T. Ishiguro, J. Tsukamoto, and A. Takahashi, *LOW-TEMPERATURE MAGNETORESISTANCE IN FULLY-DOPED POLYACETYLENE WITH DISORDER.* Synthetic Metals, 1995. 69(1-3): p. 31-32.

5. D.-H. Ko and K. Min, *Enhancement of electrical conductivity of uniaxially and biaxially processed poly(p-phenylene sulfide) films.* Polymer Engineering & Science, 1994. 34(20): p. 1564-1579.

6. D. Zhu and M. Wu, *Highly Conductive Nano-Silver Circuits by Inkjet Printing.* Journal of Electronic Materials, 2018.

7. P. Si, J. Trinidad, L. Chen, B. Lee, A. Chen, J. Persic, R. Lyn, Z. Leonenko, and B. Zhao, *PEDOT:PSS nano-gels for highly electrically conductive silver/epoxy composite adhesives.* Journal of Materials Science: Materials in Electronics, 2018. 29(3): p. 1837-1846.

8. R. K. Goyal, K. R. Kambale, S. S. Nene, B. S. Selukar, S. Arbuj, and U. P. Mulik, *Fabrication, thermal and electrical properties of polyphenylene sulphide/copper composites.* Materials Chemistry and Physics, 2011. 128(1–2): p. 114-120.

9. P. Kar, *Recent and Future Trends of Doping in Conjugated Polymer*, in *Doping in Conjugated Polymers*,(John Wiley & Sons, Inc. 2013). p. 131-144.

10. P. Kar, *Classification of Dopants for the Conjugated Polymer*, in *Doping in Conjugated Polymers*,(John Wiley & Sons, Inc. 2013). p. 19-46.

11. B. Zong, P. Ho, and S. C. Wuang, *Synthesis and multi-applications of conductive magnetic stable polypyrrole dispersion with phase-convertible characteristics.* Materials Chemistry and Physics, 2015. 149-150: p. 156-163.

12. P. Kar, *Introduction to Doping in Conjugated Polymer*, in *Doping in Conjugated Polymers*,(John Wiley & Sons, Inc. 2013). p. 1-18.

13. S. Peng, L. Fan, C. Wei, X. Liu, H. Zhang, W. Xu, and J. Xu, *Flexible polypyrrole/copper sulfide/bacterial cellulose nanofibrous composite membranes as supercapacitor electrodes.* Carbohydrate Polymers, 2017. 157: p. 344-352.

14. M. Asyraf, M. Anwar, L. M. Sheng, and M. K. Danquah, *Recent Development of Nanomaterial-Doped Conductive Polymers.* JOM, 2017. 69(12): p. 2515-2523.

15. L. Yuan, C. Wan, X. Ye, and F. Wu, *Facial Synthesis of Silver-incorporated Conductive Polypyrrole Submicron Spheres for Supercapacitors.* Electrochimica Acta, 2016. 213: p. 115-123.

16. J. Xu, D. Wang, Y. Yuan, W. Wei, L. Duan, L. Wang, H. Bao, and W. Xu, *Polypyrrole/reduced graphene oxide coated fabric electrodes for supercapacitor application.* Organic Electronics, 2015. 24: p. 153-159.

17. Z. D. Kojabad and S. A. Shojaosadati, *Chemical Synthesis of Polypyrrole Nanotubes for Neural Microelectrodes.* Procedia Materials Science, 2015. 11: p. 147-151.

18. C. Yang, H. Mo, L. Zang, J. Qiu, E. Sakai, and X. Wu, *A facile method to synthesize polypyrrole nanoparticles in the presence of natural organic phosphate.* Physica B: Condensed Matter, 2014. 449: p. 181-185.

19. D. Sangian, W. Zheng, and G. M. Spinks, *Optimization of the sequential polymerization synthesis method for polypyrrole films.* Synthetic Metals, 2014. 189: p. 53-56.

20. X. Wu, M. Liu, and M. Jia, *Electrical conductivity of polypyrrole/expanded graphite composites prepared by chemical oxidation polymerization.* Synthetic Metals, 2013. 177: p. 60-64.

21. Y. Ali, K. Sharma, V. Kumar, R. G. Sonkawade, and A. S. Dhaliwal, *Polypyrrole microspheroidals decorated with Ag nanostructure: Synthesis and their characterization.* Applied Surface Science, 2013. 280: p. 950-956.

22. R. Yuan, H. Liu, P. Yu, H. Wang, and J. Liu, *Enhancement of adhesion, mechanical strength and anti-corrosion by multilayer superhydrophobic coating embedded electroactive PANI/CNF nanocomposite.* Journal of Polymer Research, 2018. 25(7): p. 151.

23. S. Biswas, B. Dutta, and S. Bhattacharya, *Consequence of silver nanoparticles embedment on the carrier mobility and space charge limited conduction in doped polyaniline.* Applied Surface Science, 2014. 292: p. 420-431.

24. R. Balint, N. J. Cassidy, and S. H. Cartmell, *Conductive polymers: towards a smart biomaterial for tissue engineering.* Acta Biomater, 2014. 10(6): p. 2341-53.

25. R. E. Rivero, M. A. Molina, C. R. Rivarola, and C. A. Barbero, *Pressure and microwave sensors/actuators based on smart hydrogel/conductive polymer nanocomposite.* Sensors and Actuators B: Chemical, 2014. 190: p. 270-278.

26. M. O. Jaroslav Stejskala, Svetlana Fedorovac, Jan Prokes, Miroslava Trchova, *Polyaniline and polypyrrole prepared in the presence of surfactants a comparative conductivity study.pdf.* 2003.

27. S. Imai, *Enhancing electrical conductivity and electrical thermal characteristics of a PEDOT:PSS thin layer by using solvent treatment and adding Ag nanoparticle solution.* Precision Engineering, 2015. 42: p. 143-150.

28. S. Radhakrishnan, C. Sumathi, A. Umar, S. Jae Kim, J. Wilson, and V. Dharuman, *Polypyrrole-poly(3,4-ethylenedioxythiophene)-Ag (PPy-PEDOT-Ag) nanocomposite films for label-free electrochemical DNA sensing.* Biosens Bioelectron, 2013. 47: p. 133-40.

29. A. J. Epstein, F.-C. Hsu, N.-R. Chiou, and V. N. Prigodin, *Electric-field induced ion-leveraged metal–insulator transition in conducting polymer-based field effect devices.* Current Applied Physics, 2002. 2(4): p. 339-343.

30. P. E. Gusakov, A. V. Andrianov, A. N. Aleshin, S. Matsushita, and K. Akagi, *Electrical and optical properties of doped helical polyacetylene graphite films in terahertz frequency range.* Synthetic Metals, 2012. 162(21-22): p. 1846-1851.

31. S. Radhakrishnan, S. Chakne, and P. N. Shelke, *High piezoresistivity in conducting polymer composites.* Materials Letters, 1994. 18(5): p. 358-362.

32. T. A. Skotheim, R. L. Elsenbaumer, and J. R. Reynolds, *Handbook of Conducting Polymers*. Vol. Vol. 2.(Marcel Dekker, New York: T.A. Ed. 1986.

33. H. Cartwright, *Physical Chemistry. By Peter Atkins, Oxford University Press: Oxford, U.K. xvi + 997 pp. £28.99. Includes CD. ISBN 0-19-850101-3. Student's Solutions Manual and Instructor's Solutions Manual are also available.* The Chemical Educator, 2001. 6(4): p. 262-263.

34. P. Kar, *Influence of Properties of Conjugated Polymer on Doping*, in *Doping in Conjugated Polymers*,(John Wiley & Sons, Inc. 2013). p. 81-96.

35. O. Chemistry. *Chemistry*. 2014 Apr 28, 2015 [cited 2014; Available from: https://cnx.org/contents/havxkyvS@7.11:Vd4OhCxi@3/Multiple-Bonds.

36. H. W. Hill and D. G. Brady, *Properties, environmental stability, and molding characteristics of polyphenylene sulfide.* Polymer Engineering & Science, 1976. 16(12): p. 831-835.

37. A. Kultys, *Sulfur-Containing Polymers*, in *Encyclopedia of Polymer Science and Technology*,(John Wiley & Sons, Inc. 2002.

38. J. J. T. Edmonds and J. H. W. Hill, *Production of polymers from aromatic compounds*. 1967, Google Patents.

39. L. W. Shacklette, R. L. Elsenbaumer, R. R. Chance, H. Eckhardt, J. E. Frommer, and R. H. Baughman, *Conducting complexes of polyphenylene sulfides.* The Journal of Chemical Physics, 1981. 75(4): p. 1919-1927.

40. T. C. Clarke, K. K. Kanazawa, V. Y. Lee, J. F. Rabolt, J. R. Reynolds, and G. B. Street, *Poly(P-phenylene sulfide) hexafluoroarsenate: A novel conducting polymer.* Journal of Polymer Science: Polymer Physics Edition, 1982. 20(1): p. 117-130.

41. V. V. Tcherdyntsev, L. K. Olifirov, S. D. Kaloshkin, M. Y. Zadorozhnyy, and V. D. Danilov, *Thermal and mechanical properties of fluorinated ethylene propylene and polyphenylene sulfide-based composites obtained by high-energy ball milling.* Journal of Materials Science, 2018.

42. C. Wang, Z. Li, L. Cao, and B. Cheng, *A Superhydrophilic and Anti-Biofouling Polyphenylene Sulfide Microporous Membrane with Quaternary Ammonium Salts.* Macromolecular Research, 2018.

43. H. Huang, M. Liu, Y. Li, Y. Yu, X. Yin, J. Wu, S. Chen, J. Xu, L. Wang, and H. Wang, *Polyphenylene sulfide microfiber membrane with superhydrophobicity and superoleophilicity for oil/water separation.* Journal of Materials Science, 2018. 53(18): p. 13243-13252.

44. H. Zeng and G. Ho, *Investigation on the crystalline morphologies of polyphenylene sulfide and interfacial effect in its fibre composites.* Die Angewandte Makromolekulare Chemie, 1984. 127(1): p. 103-114.

45. J. Xing, Q.-Q. Ni, B. Deng, and Q. Liu, *Morphology and properties of polyphenylene sulfide (PPS)/polyvinylidene fluoride (PVDF) polymer alloys by melt blending.* Composites Science and Technology, 2016. 134: p. 184-190.

46. G. Montaudo, C. Puglisi, and F. Samperi, *Primary thermal degradation processes occurring in poly(phenylenesulfide) investigated by direct pyrolysis–mass spectrometry*. Journal of Polymer Science Part A: Polymer Chemistry, 1994. 32(10): p. 1807-1815.

47. M. Sobkowicz-Kline, B. M. Budhlall, and J. L. Mead, *Synthetic Resins and Plastics*, in *Handbook of Industrial Chemistry and Biotechnology*, J.A. Kent, T.V. Bommaraju, and S.D. Barnicki, Editors,(Cham: Springer International Publishing. 2017). p. 1397-1462.

48. A. K. Kalkar, V. D. Deshpande, and M. J. Kulkarni, *Nonisothermal crystallization kinetics of poly (phenylene sulphide) in composites with a liquid crystalline polymer.* Journal of Polymer Science Part B: Polymer Physics, 2010. 48(10): p. 1070-1100.

49. A. Benlhachemi, J. R. Gavarri, J. Musso, C. Alfredduplan, and J. Marfaing, *HIGH-T(C) SUPERCONDUCTOR POLYMER COMPOSITES - MODELING OF ABNORMAL ELECTRICAL-PROPERTIES AT LOW-TEMPERATURE.* Physica C, 1994. 230(3-4): p. 246-254.

50. R. Taherian, *Experimental and analytical model for the electrical conductivity of polymer-based nanocomposites.* Composites Science and Technology, 2016. 123: p. 17-31.

51. A. M. Díez-Pascual, M. Naffakh, C. Marco, and G. Ellis, *Mechanical and electrical properties of carbon nanotube/poly(phenylene sulphide) composites incorporating polyetherimide and inorganic fullerene-like nanoparticles.* Composites Part A: Applied Science and Manufacturing, 2012. 43(4): p. 603-612.

52. R. Balint, N. J. Cassidy, and S. H. Cartmell, *Conductive polymers: Towards a smart biomaterial for tissue engineering.* Acta Biomaterialia, 2014. 10(6): p. 2341-2353.

53. J. Upadhyay and A. Kumar, *Investigation of structural, thermal and dielectric properties of polypyrrole nanotubes tailoring with silver nanoparticles.* Composites Science and Technology, 2014. 97: p. 55-62.

54. S. Dhibar, P. Bhattacharya, G. Hatui, and C. K. Das, *Transition metal doped poly(aniline-co-pyrrole)/multi-walled carbon nanotubes nanocomposite for high performance supercapacitor electrode materials.* Journal of Alloys and Compounds, 2015. 625: p. 64-75.

55. A. N. Sruti and K. Jagannadham, *Electrical Conductivity of Graphene Composites with In and In-Ga Alloy.* Journal of Electronic Materials, 2010. 39(8): p. 1268-1276.

56. E. Kandare, A. A. Khatibi, S. Yoo, R. Wang, J. Ma, P. Olivier, N. Gleizes, and C. H. Wang, *Improving the through-thickness thermal and electrical conductivity of carbon fibre/epoxy laminates by exploiting synergy between graphene and silver nano-inclusions.* Composites Part A: Applied Science and Manufacturing, 2015. 69: p. 72-82.

57. Y. Song, J.-L. Xu, and X.-X. Liu, *Electrochemical anchoring of dual doping polypyrrole on graphene sheets partially exfoliated from graphite foil for high-performance supercapacitor electrode.* Journal of Power Sources, 2014. 249: p. 48-58.

58. B. L. Theraja, *Modern Physics*. Vol.: S. Chand Limited 2008.

59. N. R. Thompson, *28. - SILVER*, in *The Chemistry of Copper, Silver and Gold*,(Pergamon. 1973). p. 79-128.

60. *Technical Fact Sheet –*

Nanomaterials, U. States and E.P. Agency, Editors. 2017, Office of Land and Emergency

Management (5106P): USA.

61. M. S. Silberberg, *PRINCIPLES OF GENERAL CHEMISTRY*. Vol.: McGraw-Hill 2007). p. 253-256.

62. M. H. Hebb, *Electrical Conductivity of Silver Sulfide.* The Journal of Chemical Physics, 1952. 20(1): p. 185-190.

63. B. F. G. J. A. G. Massey, N. R. Thompson, R. Davis, *The Chemistry of Copper, Silver and Gold*, ed. Comprehensive Inorganic Chemistry. Vol. Great Britain: A. Wheaton & Co, Exeter 1973.

64. M. Rubner, P. Cukor, H. Jopson, and W. Deits, *Electrically conducting poly(para-phenylene sulfide) prepared by doping with nitrosyl salts from solution.* Journal of Electronic Materials, 1982. 11(2): p. 261-72.

65. N. S. Murthy, R. L. Elsenbaumer, J. E. Frommer, and R. H. Baughman, *Structural changes during annealing and during acceptor doping of oriented poly(p-phenylene sulfide).* Synthetic Metals, 1984. 9(1): p. 91-96.

66. S. Tokito, T. Tsutsui, and S. Saito, *Electrical conductivity and optical properties of poly(p-phenylene sulfide) doped with some organic acceptors.* Polymer Journal, 1985. 17(8): p. 959-968.

67. S. Kazama, K. Arai, and E. Maekawa, *SO3-doped poly(p-phenylene sulphide) I: A study of molecular structure using 1H N.M.R., 13C CP/MAS n.m.r. and i.r. spectroscopy.* Synthetic Metals, 1986. 15(4): p. 299-309.

68. C. Arbizzani, M. Mastragostino, G. Dellepiane, and P. Piaggio, *Electrochemical doping of poly(p-phenylene sulfide) in concentrated sulfuric acid.* Synthetic Metals, 1992. 51(1): p. 63-67.

69. J. Tsukamoto, S. Fukuda, K. Tanaka, and T. Yamabe, *Conduction mechanism of doped polyphenylenesulfide.* Synthetic Metals, 1987. 17(1–3): p. 673-678.

70. D. R. Rueda, M. E. Cagiao, F. J. Balta Calleja, and J. M. Palacios, *PROPERTIES OF SbCl5-DOPED PPP/PPS COMPOSITES I. ELECTRICAL CONDUCTIVITY STUDY.* Synthetic Metals, 1987. 22(1): p. 53-61.

71. P. Hruszka, J. Jurga, J. Kubis, and N. Piślewski, *Nuclear magnetic relaxation in polyphenylene sulphide doped with FeCl3.* Polymer, 1991. 32(9): p. 1589-1592.

72. S. Radhakrishnan and S. G. Joshi, *STABILIZATION OF HIGH CONDUCTIVITY IN IODINE DOPED POLYPHENYLENE SULFIDE.* Journal of Polymer Science Part C-Polymer Letters, 1989. 27(4): p. 127-131.

73. D. Lian, J. Dai, R. Zhang, M. Niu, and Y. Huang, *Enhancing the resistance against oxidation of polyphenylene sulphide fiber via incorporation of nano TiO2SiO2 and its mechanistic analysis.* Polymer Degradation and Stability, 2016. 129: p. 77-86.

74. Y. F. Zhao, M. Xiao, S. J. Wang, X. C. Ge, and Y. Z. Meng, *Preparation and properties of electrically conductive PPS/expanded graphite nanocomposites.* Composites Science and Technology, 2007. 67(11–12): p. 2528-2534.

75. J. Yang, T. Xu, A. Lu, Q. Zhang, H. Tan, and Q. Fu, *Preparation and properties of poly (p-phenylene sulfide)/multiwall carbon nanotube composites obtained by melt compounding.* Composites Science and Technology, 2009. 69(2): p. 147-153.

76. A. Golchin, K. Friedrich, A. Noll, and B. Prakash, *Influence of counter surface topography on the tribological behavior of carbon-filled PPS composites in water.* Tribology International, 2015. 88: p. 209-217.

77. W. Luo, Q. Liu, Y. Li, S. Zhou, H. Zou, and M. Liang, *Enhanced mechanical and tribological properties in polyphenylene sulfide/polytetrafluoroethylene composites reinforced by short carbon fiber.* Composites Part B: Engineering, 2016. 91: p. 579-588.

78. Y. Tanabe and H. Shimizu, *Electronic structure of poly(p-phenylene sulfide).* Polymer Engineering & Science, 1991. 31(10): p. 717-726.

79. H. Mazurek, D. R. Day, E. W. Maby, J. S. Abel, S. D. Senturia, M. S. Dresselhaus, and G. Dresselhaus, *Electrical properties of ion-implanted poly(p-phenylene sulfide).* Journal of Polymer Science: Polymer Physics Edition, 1983. 21(4): p. 537-551.

80. S. Radhakrishnan and S. G. Joshi, *Semiconducting behavior of polyphenylene sulfide doped with ferric chloride.* Journal of Macromolecular Science - Physics, 1988. B27(2-3): p. 291-303.

81. S. Radhakrishnan. *Electrical conductivity in polyphenylene sulfide doped with ferric chloride*. in *First International Conference `Electrical, Optical and Acoustic Properties of Polymers', 5-7 Sept. 1988*. 1988. London, UK: Plastics & Rubber Inst.

82. J. Tsukamoto and K. Matsumura, *DOPING OF POLY-PARA-PHENYLENESULFIDE (PPS) WITH ALCL3, FECL3 AND TAF5.* Japanese Journal of Applied Physics Part 2-Letters, 1984. 23(8): p. L584-L586.

83. C. Shanmugapriya and G. Velraj, *Investigation on structural and electrical properties of FeCl3 doped polythiophene (PT) blended with micro and nano copper particles by mechanical mixing.* Optik - International Journal for Light and Electron Optics, 2016. 127(20): p. 8940-8950.

84. J. Y. Kim, K. Ahn, S. Y. Jeong, E. D. Jeong, J. S. Jin, J. S. Bae, H. G. Kim, and C. R. Cho, *Enhancement of adhesion between polyphenylene sulfide and copper by surface treatments.* Current Applied Physics, 2014. 14(1): p. 118-121.

85. N. S. Akbar, D. Tripathi, and O. A. Bég, *MHD convective heat transfer of nanofluids through a flexible tube with buoyancy: A study of nano-particle shape effects.* Advanced Powder Technology, 2017. 28(2): p. 453-462.

86. S. K. Das, S. U. S. Choi, and H. E. Patel, *Heat Transfer in Nanofluids—A Review.* Heat Transfer Engineering, 2006. 27(10): p. 3-19.

87. D. Wen, G. Lin, S. Vafaei, and K. Zhang, *Review of nanofluids for heat transfer applications.* Particuology, 2009. 7(2): p. 141-150.

88. M. J. Moran, H. N. Shapiro, D. D. Boettner, and M. B. Bailey, *Fundamentals of Engineering Thermodynamics, 8th Edition*. Vol.: Wiley 2014.

89. X.-G. LI, M.-R. HUANG, H. BAI, and Y.-L. YANG, *High-Resolution Thermogravimetry of Polyphenylene Sulfide Film under Four Atmospheres.* 2001.

90. M. F. Cheung, A. Golovoy, H. K. Plummer, and H. van Oene, *Polysulphone and poly(phenylene sulphide) blends: 1. Thermal characterization and phase morphology.* Polymer, 1990. 31(12): p. 2299-2306.

91. I. Kubelík and A. Tříska, *The temperature dependence of the electrical conductivity in amorphous germanium.* Czechoslovak Journal of Physics B, 1972. 22(6): p. 506-511.

Every reasonable effort had been made to acknowledge the owners of copyright material. I would be pleased to hear from any copyright owner who had been omitted or incorrectly acknowledged.